



<https://technobius.kz/>

e-ISSN
2789-7338

Technobius

A peer-reviewed open-access journal

Technobius, LLP

Volume 4, No. 3, 2024



Technobius

Volume 4, No. 3, 2024



A peer-reviewed open-access journal registered by the Ministry of Culture and Information of the Republic of Kazakhstan, Certificate № KZ26VPY00087928 dated 21.02.2024




ISSN (Online): 2789-7338

Thematic Directions: Construction, Materials Science




Publisher: Technobius, LLP

Address: 2 Turkestan street, office 116, 010000, Astana, Republic of Kazakhstan




Editor-in-Chief:




   *Yelbek Utepov*, PhD, Professor, Department of Civil Engineering, L.N. Gumilyov Eurasian National University, Astana, Kazakhstan




Technical Editor:




   *Assel Tulebekova*, PhD, Professor, Department of Civil Engineering, L.N. Gumilyov Eurasian National University, Astana, Kazakhstan




Editors:



   *Victor Kaliakin*, PhD, Professor, Department of Civil & Environmental Engineering, University of Delaware, Newark, United States




   *Askar Zhussupbekov*, Doctor of Technical Sciences, Professor, Department of Civil Engineering, L.N. Gumilyov Eurasian National University, Astana, Kazakhstan




   *Talal Awwad*, Doctor of Technical Sciences, Professor, Department of Geotechnical Engineering, Damascus University, Damascus, Syria




   *Evgeniya Tkach*, Doctor of Technical Sciences, Professor, Department of Building Materials Science, Moscow State University of Civil Engineering, Moscow, Russian Federation




   *Ignacio Menéndez Pidal de Navascués*, Doctor of Technical Sciences, Professor, Department of Civil Engineering, Technical University of Madrid, Madrid, Spain

   *Irina Aubakirova*, Candidate of Technical Sciences, Associate Professor, Department of Building Materials Technology and Metrology, Saint Petersburg State University of Architecture and Civil Engineering, Saint Petersburg, Russian Federation

   *Daniyar Akhmetov*, Doctor of Technical Sciences, Associate Professor, Department of Construction and Building materials, Satbayev University, Almaty, Kazakhstan

   *Zhanbolat Shakhmov*, PhD, Associate Professor, Department of Civil Engineering, L.N. Gumilyov Eurasian National University, Astana, Kazakhstan

   *Timoth Mkilima*, PhD, Lecturer, Department of Environmental Engineering and Management, the University of Dodoma, Dodoma, Tanzania

   *Aliya Aldungarova*, PhD, Associate Professor, School of Architecture, Civil Engineering and Energy, D. Serikbayev East Kazakhstan Technical University, Ust-Kamenogorsk, Kazakhstan

Copyright: © Technobius, LLP

Contacts: Website: <https://technobius.kz/>
E-mail: technobius.research@gmail.com

CONTENTS

Title and Authors	Category	No.
Concretes based on technogenic wastes formed during the mechanical processing of carbonate rocks <i>Raushan Nurymbetova, Rayimberdy Ristavletov, Nikolay Suzev, Elmira Kalshabekova, Ruslan Kudabayev</i>	<i>Materials Science</i>	0061
Examining intermediate soil properties variability through spatial interpolation methods in GIS <i>Aliya Aldungarova, Tymarkul Muzdybayeva, Assel Mukhamejanova, Nurgul Alibekova, Khrystyna Moskalova, Sabit Karaulov</i>	<i>Construction</i>	0062
Fractal model of the strength of lightweight concrete based on volcanic tuff taking into account the scale effect <i>Yerlan Khamza, Vladimir Selyaev, Maratbek Zhuginissov, Zhanar Zhumadilova</i>	<i>Materials Science</i>	0063
Binding properties of synthesized CS glasses activated by alkaline components <i>Bakhytzhhan Sarsenbayev, Sultan Auyesbek, Meiram Begentayev, Nuraly Sarsenbayev, Erkin Khaltursunov, Gaukhar Sauganova</i>	<i>Materials Science</i>	0064
Research of technological parameters for producing thermal insulating arbolite based on developed slag alkali binders <i>Kuanysh Imanaliyev, Baurzhan Amiraliyev, Kenzhebek Akmalaiuly, Erzhan Kuldeyev, Elmurad Yunusaliyev, Zhambul Aymenov</i>	<i>Materials Science</i>	0065



Concretes based on technogenic wastes formed during the mechanical processing of carbonate rocks

Raushan Nurymbetova*, Rayimberdy Ristavletov, Nikolay Suzev,
 Elmira Kalshabekova, Ruslan Kudabayev

Department of Building Materials and Expertise in Construction, Mukhtar Auezov South Kazakhstan University, Shymkent, Republic of Kazakhstan

*Correspondence: raushan.nurymbetova@aeuzov.edu.kz

Abstract. This article considers the possibility of using technogenic waste from the mechanical processing of Sastobe carbonate rocks as coarse and fine aggregates in the production of heavy concrete. X-ray diffractometric analysis CaCO_3 $d = (3.849-3.14-2.49-2.277-2.088-1.912-1.869 \text{ \AA}^0)$ and the endothermic peak in the temperature interval of 800-850°C in the differential-thermal analysis curve technogenic residues formed during mechanical processing of Sastobe carbonate rocks showed that it mainly consists of calcium carbonate. Studies have shown that fine and coarse aggregates based on carbonate rocks have a rough surface, which increases their specific surface area and ensures a strong bond with the cement stone. At the same time, technogenic waste contains 2-3% powder fraction up to 0.16 mm, this fraction serves as an active mineral mixture. As a result of research, the use of these wastes as fillers can reduce the consumption of traditional crushed stone and sand by 50% without reducing the physical and mechanical properties of concrete, replacing 50% of traditional fillers with technogenic fillers based on carbonate rocks, increasing the density of concrete (2490kg/m³), reducing its water absorption (0.66 %), strength (49.8 MPa) and frost resistance (F400) indicators made it possible to obtain concrete that is the same as the control sample and to reduce its cost without reducing the physical and mechanical properties of concrete and to improve the environmental conditions of the region.

Keywords: waste, carbonate rocks, concrete, fillers, physical and mechanical properties of concrete.

1. Introduction

In our country, the scope of involving of waste generated during the enrichment and processing of minerals is very low, only 20% is used as secondary raw materials, of which about 10% is used for building materials. The ability of the natural environment shows that it cannot process all the wastes of human activities, and the accumulated waste stock threatens the global pollution of the environment and the deterioration of natural ecosystems. Land restoration and return to economic use lag far behind the pace of their alienation. Therefore, the “Green economy” has become one of the most urgent issues in the world, including Kazakhstan. One of the main directions of the “Green economy” is the “Introduction of the waste management system” [1], [2].

Technogenic waste is solid, liquid, and gaseous production waste that is formed at enterprises in the process of obtaining the final product from raw materials.

Currently, there are two main approaches to decontamination of production waste, the first is to clean production facilities from harmful waste, and the second approach is the integrated use of natural resources, the development and implementation of effective production technologies that produce no or little waste. And one of the main sectors of the economy that allows efficient use of production waste is the construction industry, for example, 30 million tons of various wastes are effectively used annually in cement production alone [3].

Currently, there are more than 30 billion tons of waste in the Kazakh steppe. 6.7 billion of it is toxic, and 5 billion is mining debris. According to statistics, today only 10% of waste collected in the country is recycled, and 90% remains in the same state [4]. The construction industry has the potential to reuse 25-27% of the total volume of waste, but currently uses only about 4% of this raw material [5].

Research shows that only the southern regions of Kazakhstan, have a huge stock of waste suitable for the production of construction materials accumulated, the main stock of man-made waste is rocks, in particular, the heaps of the Lenger coal plant (more than 1 million tons), the polymetallic waste of the Ashchysai plant (182 million tons), carbonate wastes of the holding “Construction materials” (5.4 million tons), metallurgical wastes of JSC “Yuzhpolimetal” lead production (2.3 million tons), etc. [6].

Therefore, the use of mining waste in the production of construction materials and products is an urgent issue that not only reduces the cost of construction materials but also prevents environmental pollution.

An inexhaustible source of the raw material base of construction materials is the waste of the mining industry complex, including carbonate rocks. During the mechanical processing of rocks, unconditioned stone fragments of different fractions and shapes and waste in the form of highly dispersed powder are formed.

Studies show that the harmful effects of this waste spread to a region of 1.2 km, of which the accumulation of carbonate dust in the region between 150-650m is more than normal, and at the same time the pollution of the Earth's crust is at a very high level, and the main polluting components are chromium, lead, cobalt, zinc and iron [7].

Therefore, the integrated use of residues formed during the production of carbonate rocks not only reduces the cost of the resulting product but also increases the energy efficiency of production and improves the environmental situation in the region. Portland cement production is the largest use of technogenic waste from carbonate rocks. In the cement industry [8], in particular, the Mukhtar Auezov South Kazakhstan University is conducting research work on the production and study of composite slag-alkaline binders with local mineral mixtures and concrete based on them [9]. In [10] authors show that the production of mixed binders obtained by replacing a part of Portland cement clinker with highly dispersed active additives allows reducing carbon dioxide emissions to the atmosphere by 307 kg, to improve technical and economic indicators of Portland cement production.

In [11], [12] authors use limestone and its waste from mechanical processing in cement production, and as a result of studying the hydration patterns of cement based on carbonate additives, offer optimal compositions of concrete with the necessary operational properties.

However, there is a lack of research on the use of technogenic waste during rock processing of carbonate rocks in heavy concrete technology and on the study of adhesion processes in the contact zone between cement stone and calcium carbonate. Therefore, the development of the technology for decontamination of technogenic wastes generated during the mechanical processing of carbonate rocks by obtaining concretes with the necessary operational properties is an urgent issue.

The purpose of the work is to study the possibility of using technogenic waste formed during the mechanical processing of Sastobe carbonate rocks as a filler in heavy concrete and optimize the composition of heavy concrete.

2. Methods

We studied the possibility of using technogenic waste generated during the mechanical processing of Sastobe carbonate rocks in the production of construction materials and the physical-mechanical and chemical-mineralogical characteristics of selected technogenic waste.

X-ray diffractometric analyses were carried out using a Bruker D&ENDEAVOR instrument using a β filter with Cu-irradiation. Diffractogram recording conditions: U=35 kV; I=20 mA; capture Q-2Q; detector 2grd/min. Diffractogram analysis was performed using a JCDD card file, powder

diffractometric database PDF2, and diffractogram data of pure minerals without impurities. The chemical composition of the waste (SEM) was determined by the method of raster electron microscopy carried out on a JEOL-6490 LV electron microscope. All analyses were carried out in the accredited laboratory of Mukhtar Auezov South Kazakhstan University – Regional Engineering Testing Laboratory “Structural and Biochemical Materials”.

3. Results and Discussion

The results of the physicochemical analysis of technogenic residues formed during mechanical processing of Sastobe carbonate rocks are shown in Figures 1 and 2, and Table 1 below.

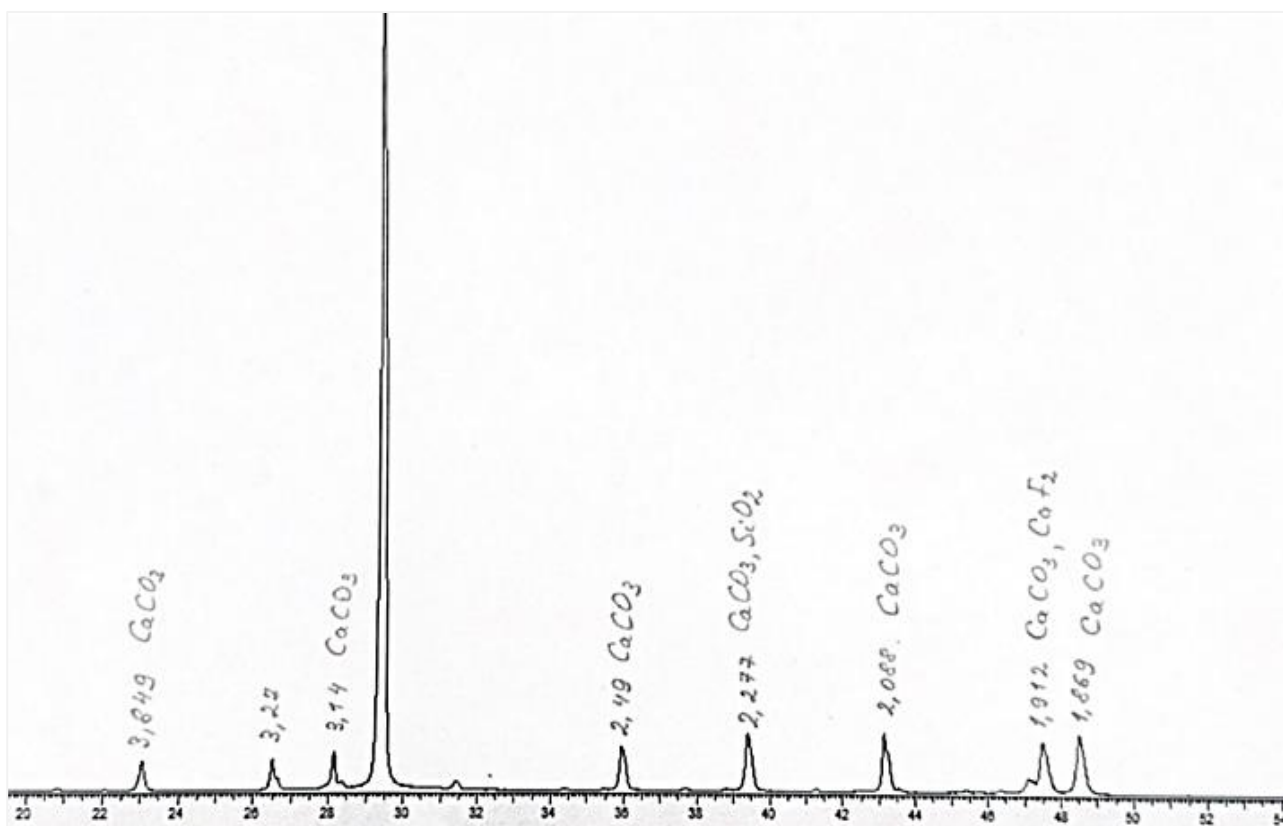


Figure 1 – X-ray diffractometric analysis results of technogenic waste

Table 1 – Results of analysis of technogenic waste by the method of raster electron microscopy

Element	Weight, %	Oxide	Weight, %
C	13.97	-	-
O	46.79	-	-
Na	0.45	Na ₂ O	0.61
Mg	0.33	MgO	0.55
Al	0.40	Al ₂ O ₃	0.76
Si	1.21	SiO ₂	2.59
S	0.44	-	-
K	0.18	K ₂ O	0.22
Ca	35.77	CaO	50.04
Fe	0.45	Fe ₂ O ₃	0.64
Total	100.00		

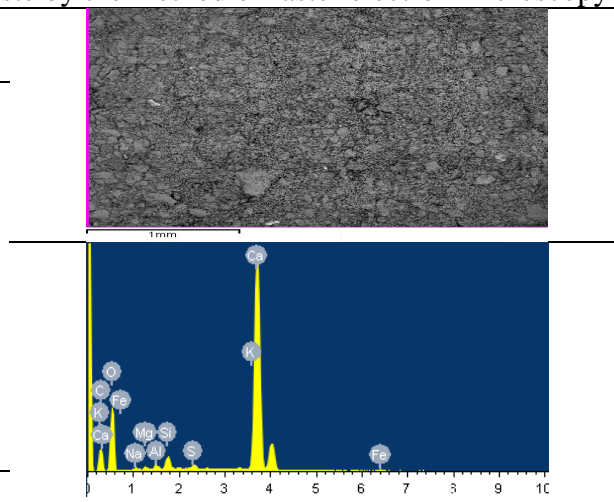
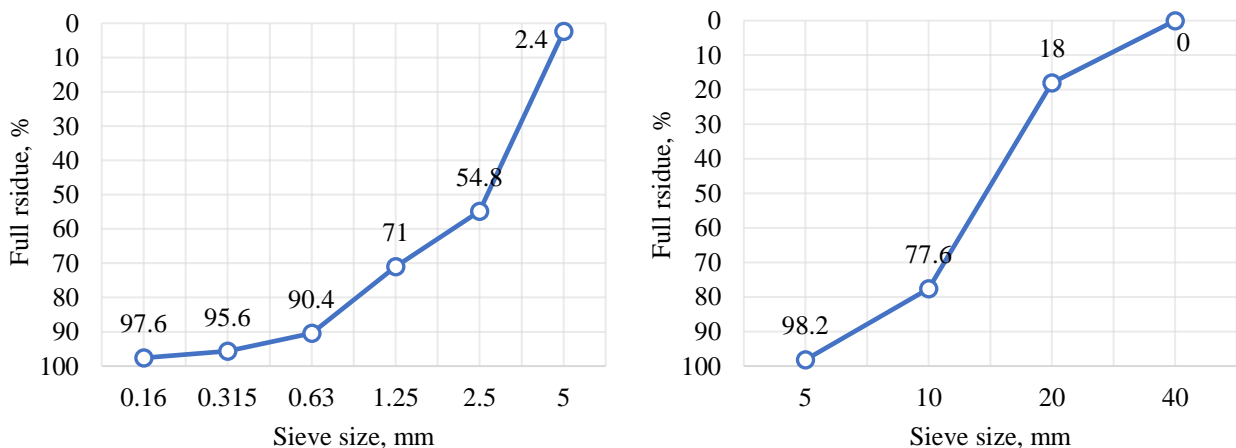




Figure 2 – Results of raster differential thermal analysis of technogenic residues formed during grinding of Sastobe carbonate rocks

The results of the physicochemical analysis show that technogenic waste formed during the mechanical processing of Sastobe carbonate rocks mainly consists of calcium carbonate CaCO_3 $d=(3.849-3.14-2.49-2.277-2.088-1.912-1.869 \text{ A}^0)$. The endothermic peak in the DTA curve in the temperature interval of 800-850°C is explained by the decomposition of the original calcium carbonate into calcium oxide with the release of carbon dioxide [13], [14]. X-ray diffractometric analysis also showed a small amount of quartzite SiO_2 $d=(2.77 \text{ A}^0)$, fluorite CaF_2 $d=(1.912 \text{ A}^0)$ minerals, and the analysis of the chemical composition of the mixture showed a small amount of sodium, magnesium, aluminum and iron compounds.

To achieve the goal set, the qualitative characteristics of man-made wastes were determined, and the possibilities of using technogenic wastes formed during the grinding of Sastobe carbonate rocks as a filler and mineral admixture in the production of heavy concrete were studied. Physical and mechanical properties of crushed stone and sand based on man-made waste were studied following the requirements of GOST 8735-88 ST RK 1217-2003 (Figure 3, Tables 2 and 3).



a) Granular composition of Sastobe carbonate waste (sand) $\mu\text{m}=4,1$

b) Granular composition of Sastobe carbonate waste (crushed stone)

Figure 3 – Granular composition of technogenic waste

Table 2 – Main characteristics of sand based on technogenic wastes formed during grinding of Sastobe carbonate rocks

Magnitude modulus	Intergranular cavity, %	True density, kg/m ³	Bulk density, kg/m ³
4.1	42.5	2220	1276

Table 3 – Characteristics of crushed stone based on technogenic wastes formed during crushing of Sastobe carbonate rocks

Cavity	True density, kg/m ³	Bulk density, kg/m ³	Grinding mark
42.5	2500	3300	M800

Studies have shown that fine and coarse aggregates based on carbonate rocks have a rough surface, which increases their specific surface area and ensures a strong bond with the cement stone. At the same time, it can be seen from the data of Figure 3 that technogenic waste contains 2-3% powder fraction up to 0.16 mm, this fraction serves as an active mineral mixture.

The use of such a fine fraction in concrete destroys all weak bonds with cement stone and leads to the formation of very strong, energetically strong homogeneous micro-particles. The smaller the size of the particles of the fine fraction during waste grinding, the more thermodynamically active they become. Micropowders are integrated into the concrete structure and increase the specific surface of cement particles [15].

Tables 4 and 5 show the qualitative indicators of fine and coarse aggregates based on technogenic waste generated during the grinding of Sastobe carbonate rocks.

Table 4 – Qualitative indicators of crushed stone based on technogenic waste formed during grinding of Sastobe carbonate rocks

Total residue on the sieve (%), mm				Intergranular cavity, %	True density, kg/m ³	Bulk density, kg/m ³	Grinding mark
5	10	20	40				
95.6	56.6	10.8	-	47.5	2500	1312	D600
90-100	30-60	≤10	≤0.5	≤48	2500	1800	≥D400

Table 5 – Qualitative indicators of sand based on technogenic waste generated during crushing of Sastobe carbonate rocks

Total residue on the sieve (%), mm						Magnitude modulus	Intergranular cavity, %	True density, kg/m ³	Bulk density, kg/m ³
5	2.5	1.25	0.63	0.315	0.16				
2.4	54.8	71.0	90.4	95.6	97.6	4.1	42.5	2220	1276
15			65-75			3.5			

Studies have shown that aggregates based on technogenic waste generated during the crushing of carbonate rocks meet the requirements of the state standard. «Another advantage of carbonate rocks is their cheapness compared to other components of concrete, both large-grained fractions and finely dispersed particles of these wastes can be used as local raw materials for the production of concrete with improved properties, it is characterized by good workability and low density compared to other known concrete components. Depending on the properties of the carbonate composite, limestone can act in two ways: as an inert material, replacing dense and, accordingly, heavy structural elements from other minerals, and as a fine mineral filler, it can act chemically concerning cement stone [13].

For further studies, the composition of heavy concrete was selected by replacing a certain part of natural aggregates with waste-based aggregates.

Tables 6 and 7 show concrete compositions replaced by 25%, 50%, and 100% man-made waste of traditional fillers and the main physical and mechanical properties of concrete mix and concrete.

Table 6 – Composition of concrete with fillers based on technogenic waste formed during grinding of Sastobe carbonate rocks

Composition of concrete	Cement	Crushed stone	Sand	Water
Concretes based on traditional aggregates	432	1200	720	182
Composition of Sastobe carbonate waste 25%	432	300	180	182
Composition of Sastobe carbonate waste 50%	432	600	360	182
Composition of Sastobe carbonate waste 100%	432	1200	720	182

Table 7 – Effect of technogenic aggregates on the main characteristics of the concrete mixture

Concrete mix composition	Movability(cm)
Concretes based on traditional aggregates	8
Composition of Sastobe carbonate waste 25%	6
Composition of Sastobe carbonate waste 50%	5
Composition of Sastobe carbonate waste 100%	3

The study of the effect of fine and coarse aggregates based on carbonate waste on the main characteristics of the concrete mixture showed that the water demand of the mixture gradually increases as the proportion of technogenic waste increases. If the W/C ratio is the same, as the proportion of waste increases, the rigidity of the concrete mixture increases, which is explained by the high specific surface area and porosity of non-conditioned aggregates.

It was found that the technogenic waste has no significant effect on the concrete density, as shown in Figure 4, the complete replacement of aggregates with waste from the mechanical processing of carbonate rocks increases the density of concrete by 2% compared to the control composition. This is mainly because the fine fraction in the carbonate waste increases the volume of the cement paste and fills the pores and interspaces of the filler.

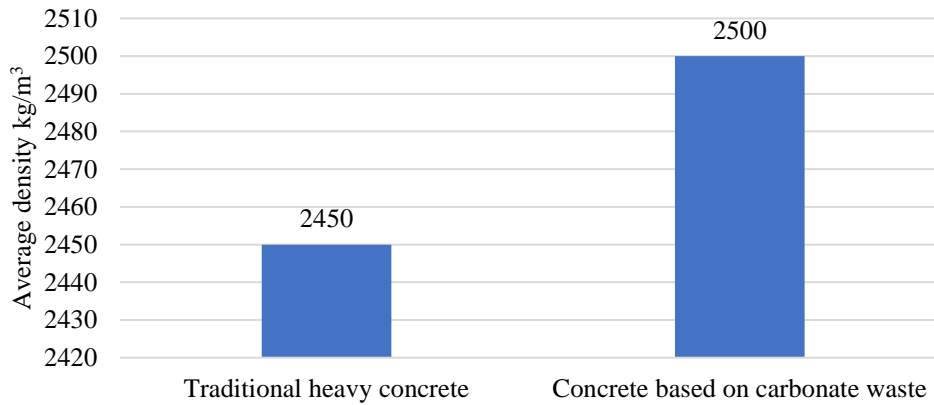


Figure 4 – Density of concrete with aggregates based on technogenic wastes formed during grinding of Sastobe carbonate rocks

Table 8 and Figure 5 show the effect of technogenic aggregates on the strength gain kinetics of concrete

Table 8 – Effect of technogenic aggregates on the kinetics of strength gain of concrete

Concrete composition	Strength 7 days, MPa	Strength 14 days, MPa	Strength 28 days, MPa
0	33.7	51.4	51.7
1	32.7	34.1	32.1
2	33.6	45.8	49.8
3	29.6	37.0	49.5

Compared to the control sample, the strength gain kinetics of the samples based on man-made aggregates is somewhat lower, however, the strength gain kinetics and the tensile strength of the samples replaced with 50% man-made waste were found to be close to the control sample.

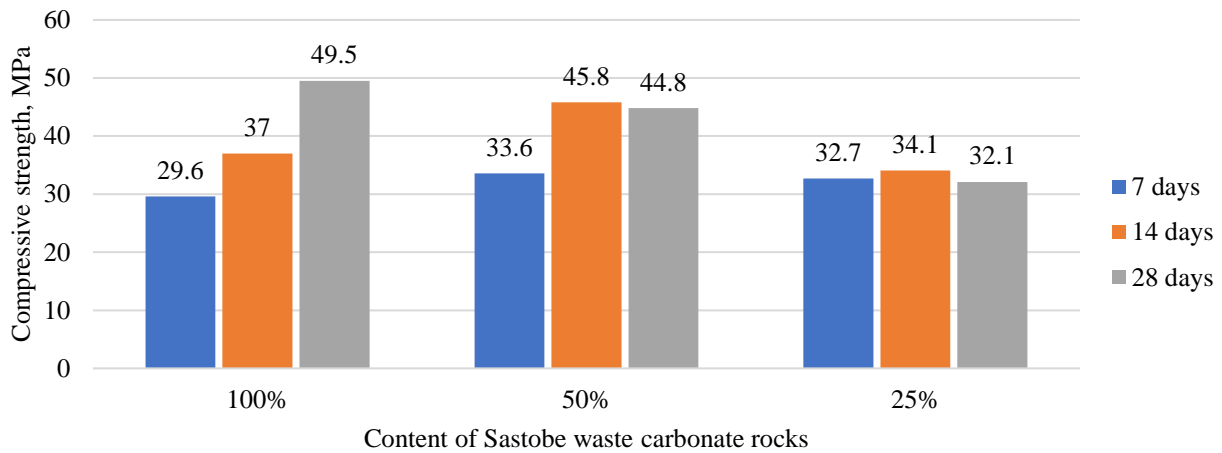


Figure 5 – Effect of technogenic aggregates on the strength gain kinetics of concrete

Authors of the works [16] show that “hardening cement paste based on Portland cement forms calcium carbonate of different composition in $\text{CaCO}_3\text{-Ca(OH)}_2\text{-H}_2\text{O}$ system when reacting with carbonate filler. It is noted that calcium carbonate crystals are relatively small in size and can be freely located among hydration products, different from Ca(OH)_2 crystals.

According to Table 4, used technogenic waste contains 2-3% highly dispersed (0.16 sieved) waste. Based on the data of this work [17], it affects the chemical activity of carbonate rocks, and in the “carbonate-cement” system, calcium hydrocarboaluminate $3\text{CaO}\cdot\text{Al}_2\text{O}_3\cdot\text{CaCO}_3\cdot 11\text{H}_2\text{O}$, hydrocarbonate – $\text{CaCO}_3\text{-Ca(OH)}_2\cdot\text{H}_2\text{O}$, and hydrosulfocarboasilicate (thaumasite) $\text{CaO}\cdot\text{SiO}_2\cdot\text{CaSO}_4\cdot\text{CaCO}_3\cdot 15\text{H}_2\text{O}$ is formed.

Figure 6 shows an electronic image of the contact area between cement stone and carbonate aggregate.

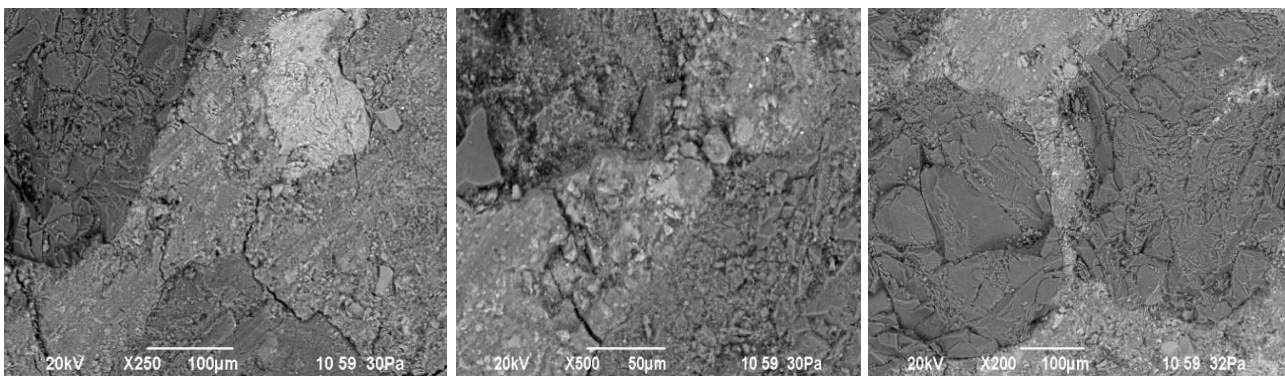


Figure 6 – Electron image of the cement stone and carbonate aggregate contact zone

As can be seen from Figure 8, due to the roughness of the surface of the fillers, close contact adhesion is observed, as well as traces of calcium carbonate formed as a result of the carbonization of calcium hydroxide.

In general, the adhesion strength of the aggregate to the cement stone is a determining factor of the overall strength of the concrete. According to the data of the work [18], the adhesion strength of cement stone with filler grains depends on several factors, namely, the shape, roughness, and cleanliness of the filler grains, the chemical and mineralogical composition of the filler grains, the strength of the cement stone, the presence of mineral additives that increase the adhesion strength, micro defects of the structure in the contact area.

Table 9 shows the physical and mechanical properties of concrete based on technogenic aggregates formed during the grinding of Sastobe carbonate rocks.

Table 9 – Physical and mechanical properties of concrete based on technogenic aggregates

Concrete composition	Density kg/m ³	Water absorption, W%	Frost resistance (F), cycles
0	2450	0.67	F400
1	2500	0.98	F300
2	2490	0.66	F400
3	2550	0.73	F200

The frost resistance of the samples was determined by the accelerated method, the frost resistance of the concrete can be increased by reducing the W/C ratio and increasing the proportion of closed pores in the concrete body by adding air-entraining admixtures. In our case, as a result of an increase in the concrete density due to the deep penetration of the cement paste into the filler grains, the water absorption of the concrete decreases, and the frost resistance of the sample increases.

4. Conclusion

1. Technogenic waste formed during mechanical processing of Sastobe carbonate rocks mainly consists of calcium carbonate CaCO_3 $d=(3,849-3,14-2,49-2,277-2,088-1,912-1,869 \text{ A}^0)$, in addition, of a small amount of quartzite SiO_2 $d=(2,77 \text{ A}^0)$, fluorite CaF_2 $d=1.912 \text{ A}^0$ minerals, a small amount of sodium, magnesium, aluminum and iron compounds.

2. It was found that the use of technogenic waste formed during the mechanical processing of carbonate rocks as a filler allows to reduce the consumption of traditional crushed stone and sand by 50% without reducing the physical and mechanical properties of concrete.

3. Studies have shown that the replacement of 50% of traditional aggregates with technogenic aggregates based on carbonate rocks increased the density of concrete to 2490 kg/m³, decreased its water absorption to 0.66%, increased its compressive strength to 49.8 MPa, and frost resistance to F400, which was the same as the control sample.

4. The use of technogenic aggregates formed during the mechanical processing of carbonate rocks in heavy concrete technology allows for a reduction in the cost of concrete. It improves the environmental condition of the region without reducing the physical and mechanical properties of concrete.

References

- [1] Adilet.kz, “O Koncepcii perehoda Respubliki Kazahstan k ustojchivomu razvitiyu na 2007-2024 gody.” Accessed: Sep. 13, 2024. [Online]. Available: <https://adilet.zan.kz/rus/docs/U060000216>
- [2] B. T. Taimasov, N. N. Zhanikulov, and A. R. Kaltai, “Mineralno-syrevye istochniki dlya energosberegayushego proizvodstva portlandcementnogo klinkera,” *Complex use of mineral resources*, no. 2, pp. 95–101, 2016.
- [3] MEMR RK, “Metodicheskoe rukovodstvo po izucheniyu i ocnke tehnogennyh mineralnyh obektov, predstavlyaemyh na gosudarstvennyu ekspertizu nedr.” Accessed: Sep. 13, 2024. [Online]. Available: https://online.zakon.kz/Document/?doc_id=31371775&pos=3;-108#pos=3;-108
- [4] New Times.kz, “«Bomba zamedlennogo dejstviya»: Kazahstan nakopil bolee 32 mlrd tonn musora.” Accessed: Sep. 13, 2024. [Online]. Available: <https://newtimes.kz/obshchestvo/140999-bomba-zamedlennogo-deistviia-kazahstan-nakopil-bolee-32-mlrd-tonn-musora>
- [5] V. K. Kokunko, “Sozdaniye i razvitije syrevoj bazy stroitelnyh materialov na osnove poputnodobyvaemyh porod i othodov gorno-rudnyh predpriyatij,” *Stroitelnye materialy*, no. 4, pp. 4–6, 1994.
- [6] N. Sarsenbaev *et al.*, “Influence of additives of barium-carbonate tailing wastes on the properties of compositional binders and concretes,” *Bulletin of Belgorod State Technological University named after. V. G. Shukhov*, vol. 4, no. 4, pp. 24–31, Apr. 2019, doi: 10.34031/article_5cb1e6606f9c29.67138287.
- [7] I. I. Kosinova and M. G. Zaridze, “Geoindikatory preobrazovaniya gruntov zony aeracii v rajonah infrastruktury po dobyche i pererabotke karbonatnogo syrja,” in *Perspektivy razvitiya inzhenernyh izyskanij v stroitelstve v Rossijskoj Federacii : OAO “PNIIS” - 50 let : materialy 9-j obsherosijskoj konferencii izyskatelskih organizacij, 28-29 noyab. 2013 g.*, Moscow: OAO “PNIIS,” 2013, pp. 174–176.

- [8] R. Z. Rahimov, U. H. Magdeev, and V. N. Yarmakovskij, “Ekologiya, nauchnye dostizheniya i innovacii v proizvodstve stroitelnykh materialov na osnove i s primeneniem tehnogennoho syrya,” *Stroitelnye materialy*, no. 12, pp. 8–11, 2009.
- [9] B. K. Sarsenbaev, “Tehnologiya proizvodstva shlakoshelochnykh vyazhushih, betonov i izdelij: material tehnikeskoj informacii,” *Novosti nauki Kazahstana*, pp. 95–99, 2004.
- [10] G. V. Calder and T. D. Stark, “Aluminum Reactions and Problems in Municipal Solid Waste Landfills,” *Practice Periodical of Hazardous, Toxic, and Radioactive Waste Management*, vol. 14, no. 4, pp. 258–265, Oct. 2010, doi: 10.1061/(ASCE)HZ.1944-8376.0000045.
- [11] V. S. Demyanova, V. M. Trostyanskij, and O. A. Chumakova, “Ekologicheskie aspekty resursosberezheniya nerudnykh poleznykh iskopaemykh,” *Uspehi sovremennogo estestvoznaniya*, no. 8, pp. 91–93, 2008.
- [12] N. A. Suzev, T. M. Hudyakova, and S. A. Nekipelov, “Nekotorye svojstva betonov na karbonatnom portlandcemente,” *Tehnologii betonov*, no. 9–10, pp. 20–22, 2009.
- [13] A. U. Shayahmetov, A. G. Mustafin, and I. A. Massalimov, “Osobennosti termicheskogo razlozheniya oksida, peroksida, gidroksida i karbonata kalciya,” *Vestnik Bashkirskogo universiteta*, vol. 16, no. 1, pp. 29–32, 2011.
- [14] G. G. Islamova, T. Z. Lygina, and A. M. Gubajdullina, “Kinetika tverdogaznogo sinteza silikatov kalciya i kachestvennaya diagnostika produktov sinteza,” *Vestnik Kazanskogo tehnologicheskogo universiteta*, no. 8, pp. 257–262, 2010.
- [15] R. Arora *et al.*, “Potential utilization of waste materials for the production of green concrete: A review,” *Mater Today Proc.*, vol. 69, pp. 317–322, 2022, doi: 10.1016/j.matpr.2022.08.542.
- [16] O. V. Kononova and V. D. Cherepov, “Carbonate rocks crushing screenings based artificial stone structure formation,” *Fundamental Research*, no. 9, pp. 1200–1204, 2014.
- [17] O. V. Kononova, V. D. Cherepov, and N. A. Ivanov, “Polimercementnye kompozicii na osnove karbonatnykh porod,” in *Materialy Vserossijskoj mezhdisciplinarnoj nauchnoj konferencii «Chetyrnadcatye Vavilovskie chteniya. Rossiya v globalnom mire: vyzovy i perspektivy razvitiya»*, Yoshkar-Ola, 2011, pp. 175–178.
- [18] A. E. Shejkin, Yu. V. Chehovskij, and M. I. Brusser, *Struktura i svojstva cementnykh betonov*. Moscow: Strojizdat, 1979.

Information about authors:

Raushan Nurymbetova – PhD Student, Department of Building Materials and Expertise in Construction, Mukhtar Auezov South Kazakhstan University, Shymkent, Republic of Kazakhstan, raushan.nurymbetova@aeuzov.edu.kz

Rayimberdy Ristavletov – Candidate of Technical Sciences, Associate Professor, Department of Building Materials and Expertise in Construction, Mukhtar Auezov South Kazakhstan University, Shymkent, Republic of Kazakhstan, r.ristavletov@aeuzov.edu.kz

Nikolay Suzev – Candidate of Technical Sciences, Professor, Department of Building Materials and Expertise in Construction, Mukhtar Auezov South Kazakhstan University, Shymkent, Republic of Kazakhstan, nikolai.suzev@aeuzov.edu.kz

Elmira Kalshabekova – Candidate of Technical Sciences, Associate Professor, Department of Building Materials and Expertise in Construction, Mukhtar Auezov South Kazakhstan University, Shymkent, Republic of Kazakhstan, elmira.kalshabekova@aeuzov.edu.kz

Ruslan Kudabayev – MSc, Senior Lecturer, Department of Building Materials and Expertise in Construction, Mukhtar Auezov South Kazakhstan University, Shymkent, Republic of Kazakhstan, kudabaev_81@mail.ru

Author Contributions:

Raushan Nurymbetova – data collection, testing.

Rayimberdy Ristavletov – conceptualization, formal analysis.

Nikolay Suzev – methodology, validation, writing-review, editing.

Elmira Kalshabekova – writing-review & editing.

Ruslan Kudabayev – drafting, testing.

Conflict of Interest: The authors declare no conflict of interest.

Use of Artificial Intelligence (AI): The authors declare that AI was not used.

Received: 21.07.2024

Revised: 11.09.2024

Accepted: 12.09.2024

Published: 13.09.2024



Copyright: @ 2024 by the authors. Licensee Technobius, LLP, Astana, Republic of Kazakhstan. This article is an open access article distributed under the terms and conditions of the Creative Commons Attribution (CC BY-NC 4.0) license (<https://creativecommons.org/licenses/by-nc/4.0/>).



Examining intermediate soil properties variability through spatial interpolation methods in GIS

Aliya Aldungarova^{1,2}, Tymarkul Muzdybayeva³, Assel Mukhamejanova^{1,3*},
 Nurgul Alibekova³, Khrystyna Moskalova⁴, Sabit Karaulov¹

¹Solid Research Group, LLP, Astana, Kazakhstan

²Department of Mining, Construction and Ecology of S. Sadvakasov Agrotechnical Institute of Kokshetau University named after Sh. Ualikhanov, Kokshetau, Kazakhstan

³Department of Civil Engineering, L.N. Gumilyov Eurasian National University, Astana, Kazakhstan

⁴Department Department for Research and Development, Development and Training Centre for the Metal Industry, Metal Centre Čakovec, Čakovec, Croatia

*Correspondence: assel.84@list.ru

Abstract. This study compares Kriging and Inverse Distance Weighting (IDW) spatial interpolation methods for estimating intermediate soil properties at a construction site in Astana, Kazakhstan. Using data from eight boreholes, seven engineering geological elements (EGE) were identified and analyzed at 6.5 m and 11.5 m depths. Kriging produced deformation modulus values ranging from -0.29 to 18.99 MPa at 6.5 m and -0.51 to 23.94 MPa at 11.5 m, capturing more spatial variability compared to IDW, which provided ranges of 3.3 to 18.99 MPa and 2.6 to 23.99 MPa, respectively. Kriging's ability to account for spatial correlations resulted in more accurate predictions, particularly in areas with complex subsurface variability. Meanwhile, IDW offered reliable localized results, effective in more uniform geological conditions. The findings demonstrate that both methods are valuable for geotechnical applications, with the choice depending on data density and site variability.

Keywords: Kriging, Inverse Distance Weighting, underground space, spatial interpolation, GIS, intermediate characteristics, foundation bearing capacity.

1. Introduction

In the process of urban infrastructure development, the study and analysis of the geological structure of the base of buildings and structures, as well as the overall optimal use of underground space, are of great importance [1], [2]

To ensure the strength and stability of the foundations, as well as to prevent the foundation from shifting on the footings and overturning, the bearing capacity of the foundations is calculated [3]. This calculation includes determining the design load on the foundation and the ultimate resistance force of the foundation [4]. The latter depends on the mechanical and strength properties of the soil, which are determined experimentally [5].

Currently, data from point excavations made at a specific depth and location are often used for calculations [6]. However, due to limited time and financial resources, the number of such excavations may be insufficient to fully analyze the subsurface. This makes it difficult to interpret the results correctly and can lead to a situation where layers of soil with low-strength characteristics are left unaccounted for between excavations. Such layers are difficult to account for or predict with existing data analysis methods. In this regard, it is important to properly account for, i.e., it is necessary to find intermediate mechanical characteristics of the soil to accurately predict settlement and ensure stability and strength of the foundations of buildings and structures.

The use of GIS is one of the key ways of exploring underground space [7]. GIS algorithms allow predicting values at unselected locations based on nearby measured data. Spatial interpolation methods in GIS are widely used in the world practice to obtain accurate values of geological characteristics of underground space [8], [9] The performance of these methods depends on several factors such as sample density, spatial distribution of the sample, data clustering, surface type, data variance, normality of data distribution, quality of archival information, data stratification, and grid resolution.

The [10] compared two interpolation methods, conventional Kriging and IDW, for groundwater quality assessment in the Lucknow district. The study identified high-risk areas with nitrate concentrations exceeding the permissible limits. The results of the analysis showed that the Ordinary Kriging method showed more accurate estimates compared to the IDW method.

The [11] discusses using multivariate analysis and geographic information systems for modeling and mapping foundation strength and land suitability in arid areas. The study used the IDW method in the ArcGIS 10.4 program to construct interpolation maps of soil properties.

The study [12] analyzed the effectiveness of interpolation methods such as IDW, ordinary Kriging, and co-Kriging for predicting soil properties in saline areas of northern China. The results confirmed that different methods provide similar spatial distributions of soil properties. However, the Kriging and co-Kriging methods showed more homogeneous results than the IDW method, indicating their higher accuracy and ability to account for the spatial autocorrelation of the data.

In this paper [13], an improved Kriging method was proposed, with the addition of spectral variables from high-resolution remote sensing images to the interpolation algorithm. This method was analyzed and compared with the traditional OK, co-Kriging, and KED algorithms. Applying the new algorithm to the soil moisture data produced soil moisture maps with a 30 m spatial resolution.

Thus, the study showed the need for further analysis and evaluation of spatial interpolation methods, such as IDW and Kriging, to determine intermediate geotechnical soil characteristics. Particular attention should be paid to identifying and accounting for soil layers with low-strength properties, which is critical to ensure the reliability and stability of the foundations of buildings and structures.

This study aims to compare IDW and Kriging spatial interpolation methods for determining intermediate geotechnical soil characteristics with a focus on optimizing their use in conditions of limited data, which may improve the accuracy of predictions and the safety of urban infrastructure.

2. Methods

The investigated territory is located in the capital of the Republic of Kazakhstan Astana City, located on the steppe plain in the central part of the territory of the Republic of Kazakhstan.

A distinctive feature of the climate of the Astana city territory is its sharp continentality, which is expressed in low precipitation, and significant amplitude between absolute maximum and minimum air temperatures.

Groundwater is confined to multigrained sands at the bottom of the layer with gravel and pebbles. The thickness of water-bearing sediments is 3-6 meters. From the surface, water-bearing deposits are overlapped with loams and clays with thicknesses of 2-4 meters. The main collectors of groundwater on the territory of the city are:

- aquifer in undivided alluvial alluvial sandy-gravel quaternary deposits of the Ishim River valley.
- water-bearing zone of fractured Ordovician rocks. Normative frost depth for Astana is 1.71 m (for loams and clays), 2.08 m (for sandy loams, sands, fine and dusty), 2.23 m (for gravelly, coarse, and medium sands) 2.53 m (for coarse clastic soils).

The average annual relative humidity is 67%. A topographic survey of the construction site is shown in Figure 1.



Figure 1 – Topographic survey of the construction site [14]

The figure shows the topographic survey of the investigated object. For the projected residential complex were drilled 8 wells with a maximum depth of 24 meters. Geomorphologically, the territory is confined to the left-bank floodplain terrace of the Ishim River. Groundwater level at the time of survey (01.12.2021) is fixed at depths of 3.8 - 4.0 meters, at absolute levels of 348.4...348.5 meters.

Based on the field description of soils, confirmed by the results of laboratory tests, composing the survey area, the following engineering geological elements (EGE) were identified [14]:

- EGE No. 1 (aQ/III-IV) - Loam, light brown and brown, from hard to soft-plastic consistency, with carbonate inclusions, with a mixture of organic matter up to 4.15%, with interlayers of sand and loam up to 20 cm thick.

- EGE No. 2 (aQ/III-IV) - Loam, light brown and brown, from hard to fluid consistency, with carbonate inclusions, with a mixture of organic matter up to 3.88%, with interlayers of sand and loam up to 20 cm thick.

- EGE No. 3 (aQ/III-IV) - Medium coarse sand of brown and dark brown color, water-saturated, polymictic composition, with lenses of loam and interlayers of sand of different coarseness up to 20 cm thick.

- EGE No. 4 (aQ/III-IV) - Coarse, brown, and dark brown, water-saturated, polymictic sand, with sand interlayers of various sizes up to 20 cm thick.

- EGE No. 5 (aQ/III-IV) - Gravelly sand, brown and dark brown in color, water-saturated, polymictic, with interlayers of sand of different coarseness up to 20 cm thick.

- EGE No. 6 (eC/I) - Clay, burgundy-colored, hard consistency, yellow-white in places, with spots of gelation and marganization, with interlayers of loam up to 20 cm thick.

- EGE No.7 (eC/I) - Burgundy-colored loam, hard consistency, with inclusions of dresva, in some places yellow-white color, with yellowish-white color, with spots of yellowing and marganization, with clay interlayers up to 20 cm thick.

ArcGIS Geostatistical Analyst provides statistical models and tools to provide accurate and reliable estimates of phenomena in places where measurements are not available. In our case, the use of geostatistical software provides a probabilistic basis for estimating intermediate mechanical properties of the EGE because only 8 boreholes were drilled in the study area, which is insufficient to fully characterize the entire area.

To realize the finding of intermediate values of deformation modulus, angle of internal friction, and cohesion, we used data from geological studies, presented in the form of a table similar to the one in Table 1.

Table 1 – Template for survey data aggregation

No.	E_1	c_1	ϕ_1	e_1	E_2	c_2	ϕ_2	e_2	...	E_j	c_j	ϕ_j	e_j	Latitude	Longitude
1															
2															
...															
i															

Note: i and j denote ordinal numbers of wells and soil layers (from top to bottom), respectively.

Using ArcToolbox tools in the ArcGIS Pro software package, we convert the ready Excel table with XY coordinates into points that will display the position of objects on the ground according to the specified coordinates. Thus, we mark the investigated underground space, which allows us to analyze and model the geotechnical characteristics of the ground more accurately.

We used IDW and Kriging interpolation tools to determine intermediate values of soil mechanical properties. IDW refers to deterministic interpolation methods because it is directly based on measured values falling in the neighborhood of the interpolated point and on specified mathematical formulas that determine the smoothness of the resulting surface. Kriging, on the other hand, is based on statistical models that include analysis of autocorrelation (statistical relationships between measured points). Geostatistical methods not only create a surface of predicted values but also provide measures of the validity or accuracy of the predicted values.

3. Results and Discussion

Based on the EGE data, an engineering-geological section of the construction site was constructed (Figure 2).

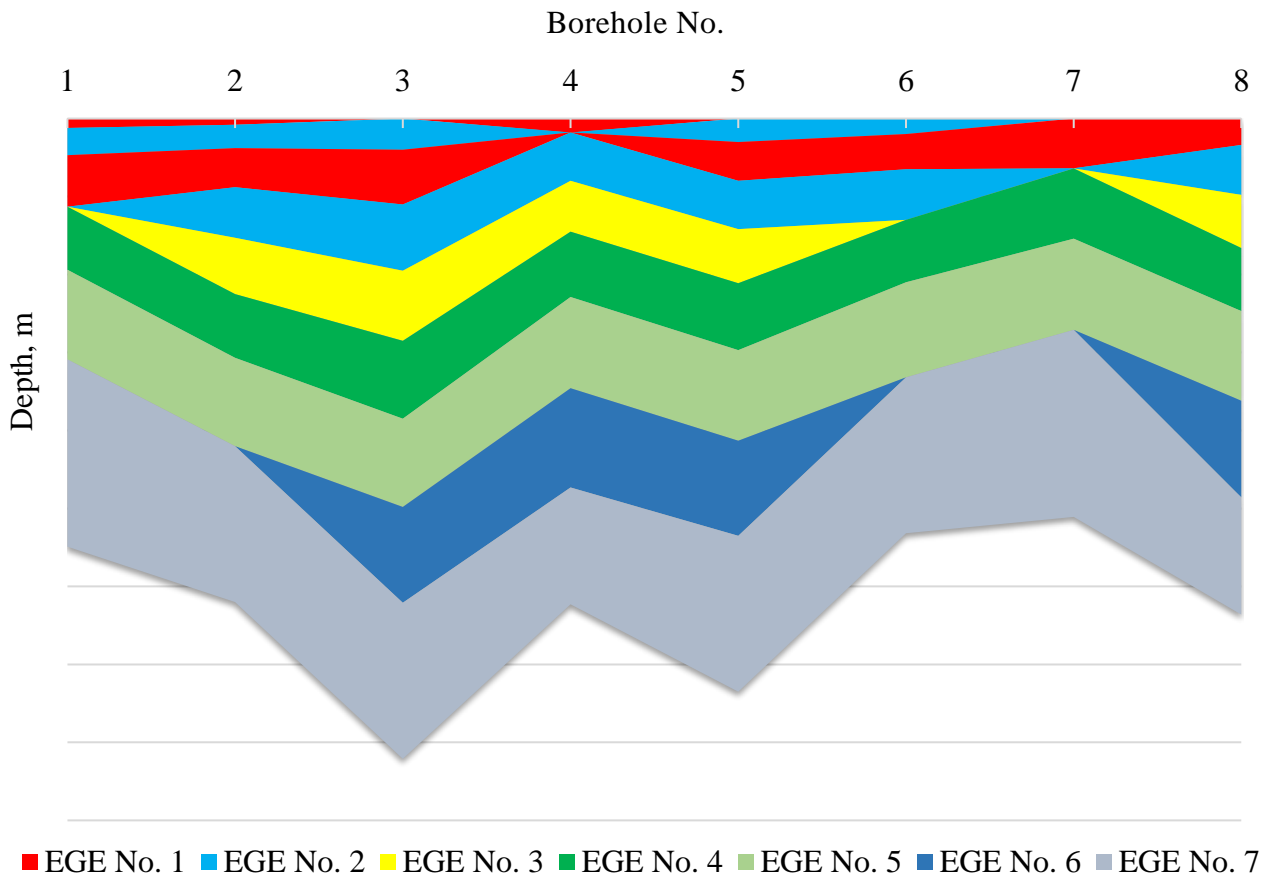


Figure 2 – Engineering-geological section

As can be seen from Figure 2, 7 EGEs were identified in 8 boreholes, ranging from loams in the upper layers, sandy soils in the middle layers, and clayey soils in the lower layers.

At a depth of 3 m, it can be seen from the visualization that layers of cohesive soils transition to non-cohesive soils, i.e., transitions from one class to another. At the same time, the opposite process is observed at a depth of 8 m: there is a transition from non-cohesive soils to cohesive soils. The lower layers of clayey soils are hard in consistency and smoothly transition to loams. In addition, several transitions are observed at greater depths. Thus, depths of 6.5 and 11.5 meters were selected for the study site (Figure 3). A raster image was plotted at these depths using ArcGIS to analyze the spatial variability of the soils in more detail.

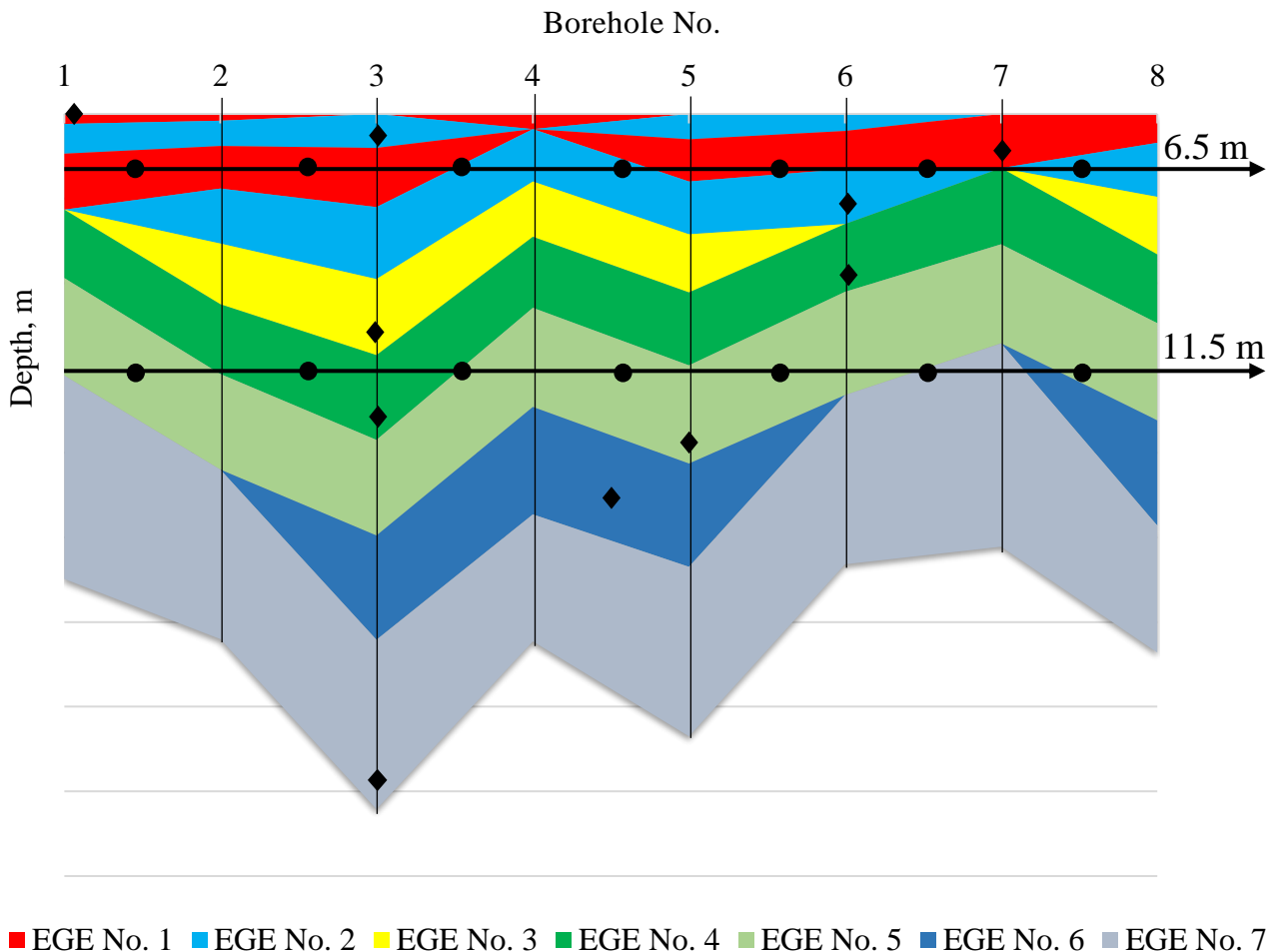


Figure 3 – Engineering-geologic section with an indication of the depth of interest

The figure above points the locations of known points in boreholes where geotechnical characteristics have been determined by conventional methods (◆), as well as unknown points between wells assumed to be determined by the new methodology (●).

Using ArcGIS capabilities, raster images were acquired at a given depth of interest (Figures 4-7). These digital images are a finite set of small discrete elements called pixels, which are organized into a two-dimensional grid.

Using interpolation algorithms and adaptive pixel size control, the number of pixels per area of the considered object using Kriging and IDW methods was 68000, with dimensions of 0.66×0.66 meters. This indicates that this approach produces a more detailed image due to the smaller pixel size, which contributes to higher accuracy and greater coverage. This is particularly important when determining unknown intermediate mechanical properties of the soil at any given location [15].

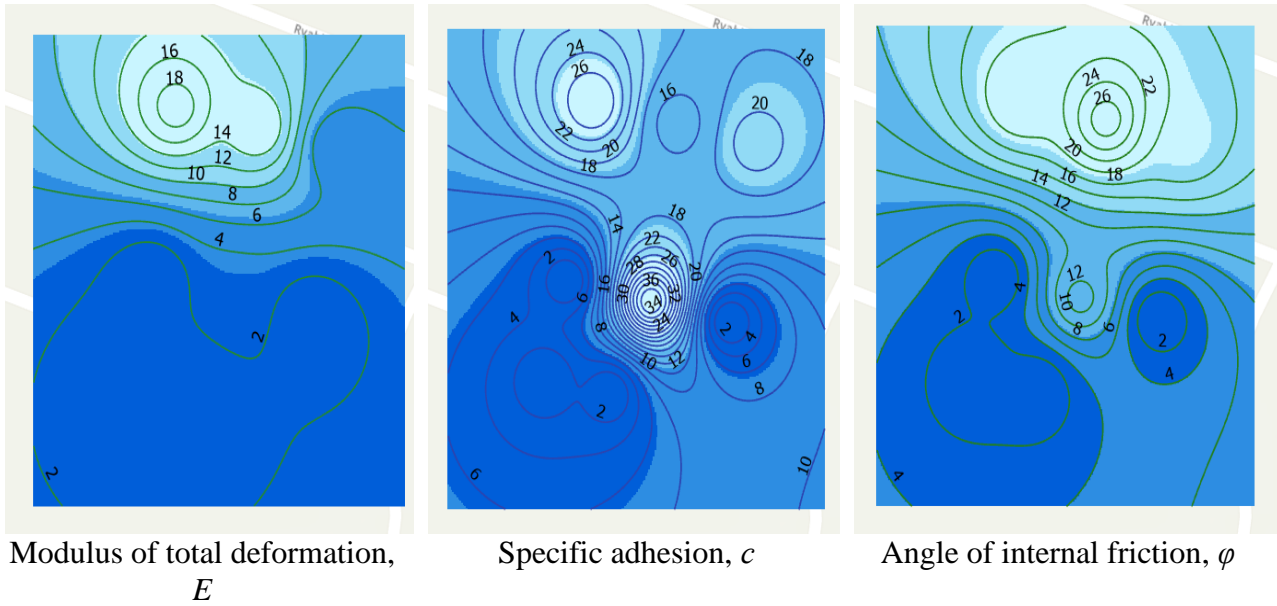


Figure 4 – Raster images of the variability of mechanical characteristics of the soil of the considered territory using the IDW interpolation method at a depth of 6.5 m

The image shows gradations with varying color shades at a depth of 6.5 m, displaying the values of various parameters. In the dark blue range, the values of total deformation modulus range from 3.3 to 10.13, specific adhesion ranges from 6.5 to 12.96, and the angle of internal friction varies from 4.02 to 14.18. In the pale blue range, the values of the total deformation modulus range from 10.13 to 18.99, specific adhesion ranges from 12.96 to 37.99, and the angle of internal friction range from 14.18 to 26.99.

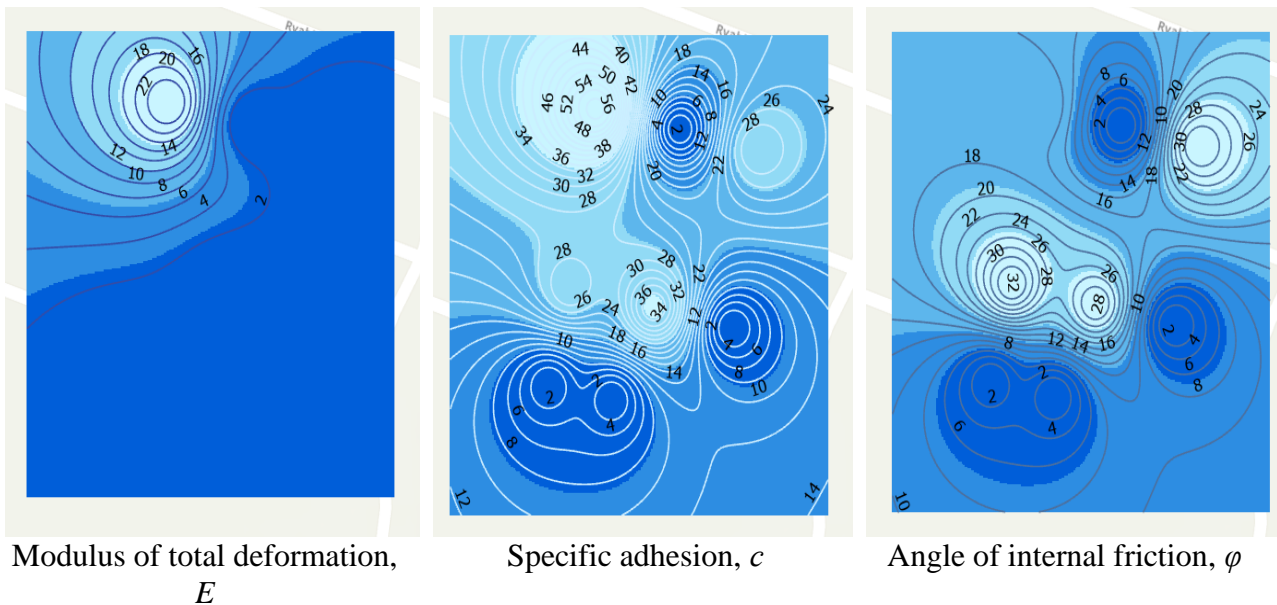


Figure 5 – Raster images of the variability of mechanical characteristics of the soil of the considered territory using the IDW interpolation method at a depth of 11.5 m

The image shows gradations with varying color shades at a depth of 11.5 m representing the values of various parameters. In the dark blue range, the values of total deformation modulus range from 2.6 to 12.04, specific adhesion ranges from 8.4 to 25.48, and the angle of internal friction varies from 6.93 to 19.19. In the pale blue range, the values of total deformation modulus range from 12.04 to 23.99, specific adhesion ranges from 25.48 to 56.99, and the angle of internal friction ranges from 19.19 to 33.99.

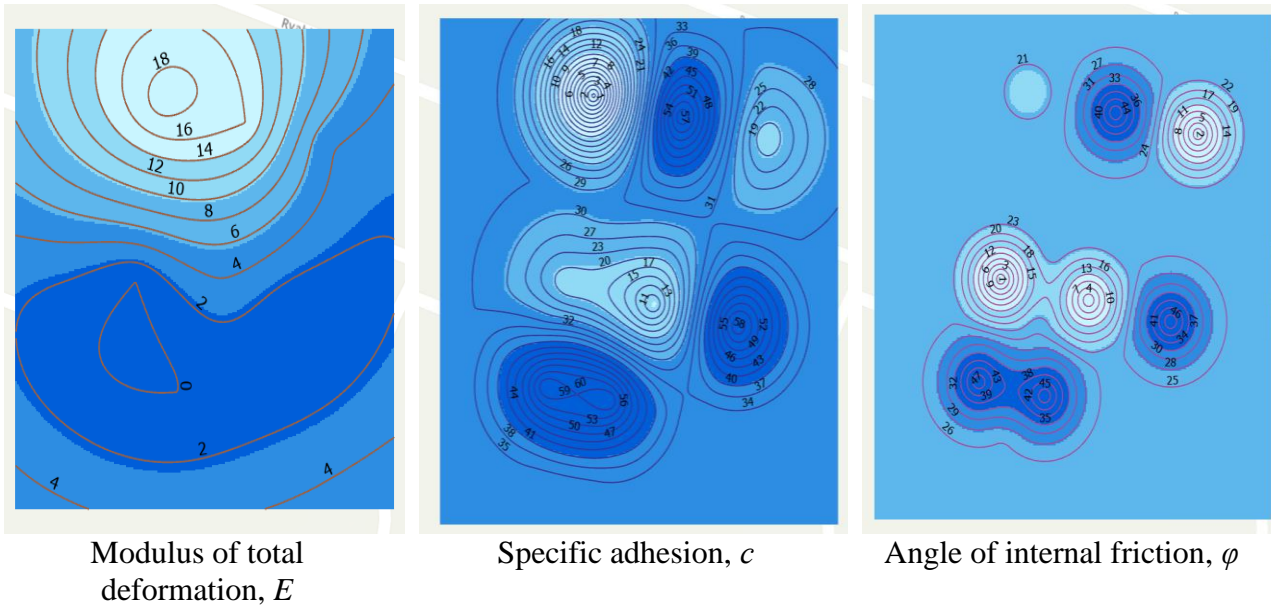


Figure 6 – Raster images of the variability of mechanical characteristics of the soil of the considered territory using the Kriging interpolation method at a depth of 6.5 m

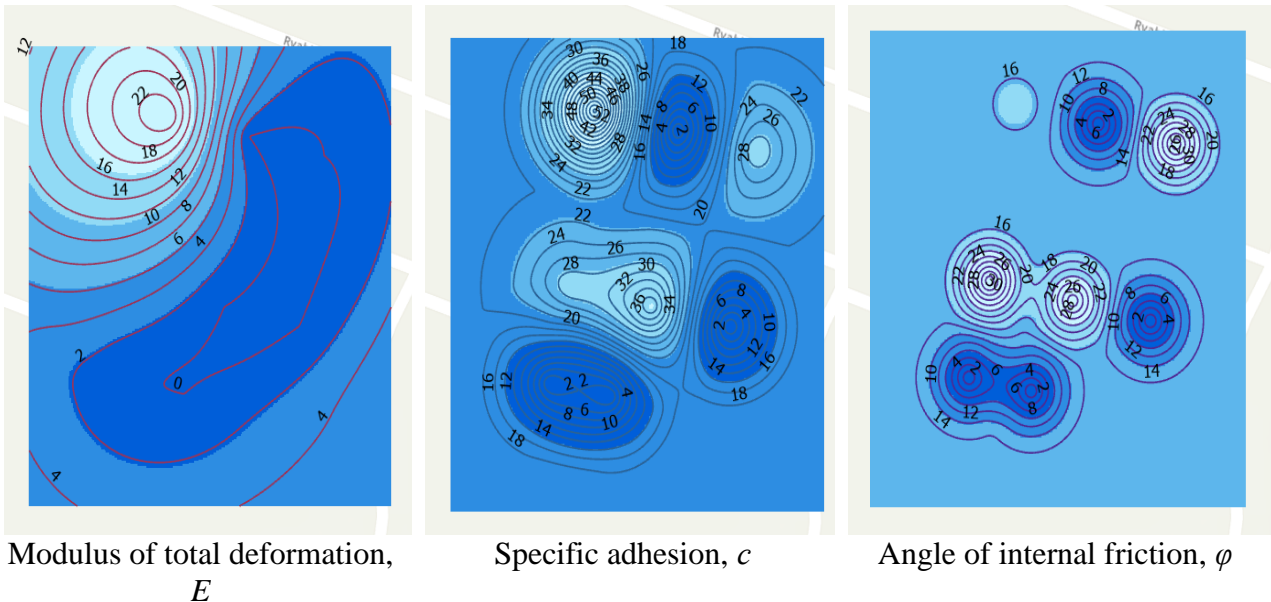


Figure 7 – Raster images of the variability of mechanical characteristics of the soil of the considered territory using the Kriging interpolation method at the depth of 11.5 m

Table 2 below demonstrates the ranges of soil parameters variability in the Kriging method.

Table 2 – Variability of soil parameters at depths of 6.5 m and 11.5 m in the Kriging method

Parameter	Dark blue range (6.5 m)	Pale blue range (6.5 m)	Dark blue range (11.5 m)	Pale blue range (11.5 m)
Modulus of total deformation, E	-0.29 to 9.69	9.69 to 18.99	-0.51 to 11.37	11.37 to 23.94
Specific adhesion, c	0.093 to 18.63	18.63 to 37.32	0.06 to 27.66	27.66 to 56.83
Angle of internal friction, φ	-0.26 to 13.72	13.72 to 26.96	0.08 to 16.39	16.39 to 33.9

Now let us consider finding intermediate characteristics at depths of 6.5 and 11.5 m, e.g., for deformation modulus (Figures 8-11).

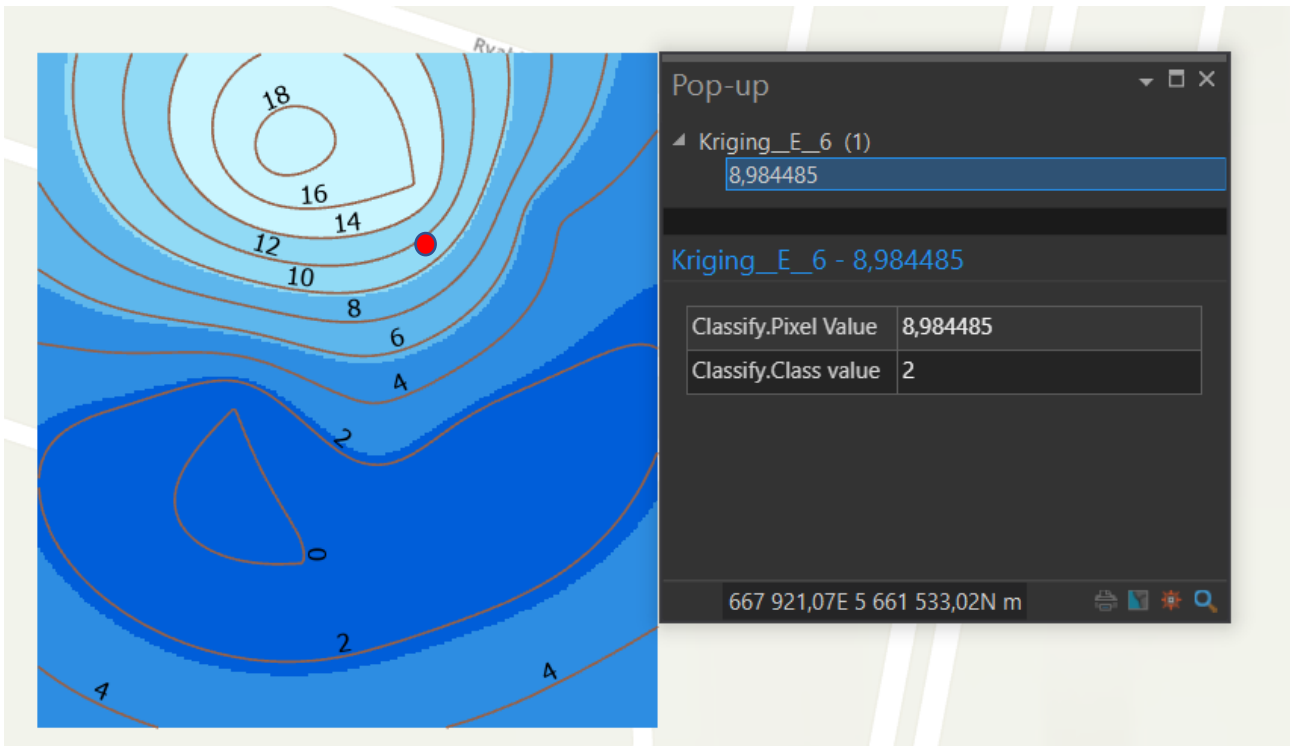


Figure 8 – Raster images of the variability of mechanical characteristics of the soil of the considered territory using the Kriging interpolation method at a depth of 6.5 m

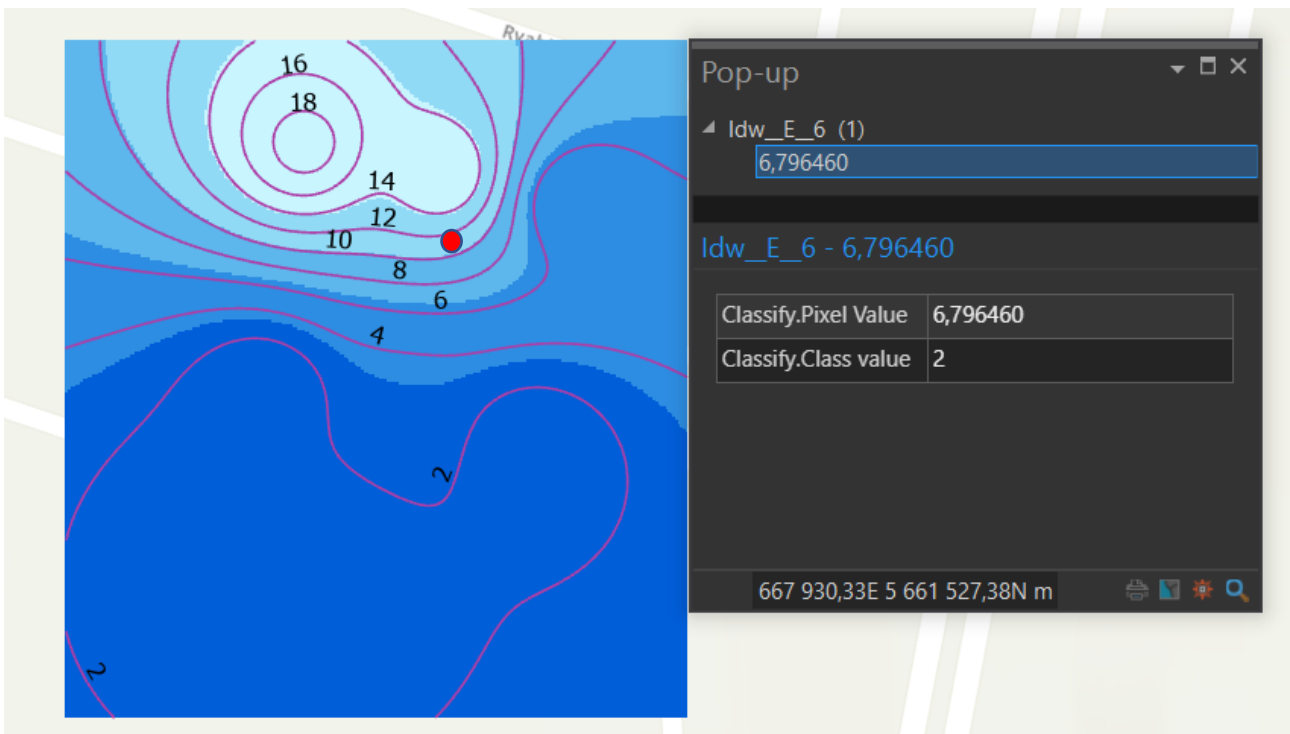


Figure 9 – Raster images of the variability of mechanical characteristics of the soil of the territory under consideration using the IDW interpolation method at a depth of 6.5 m

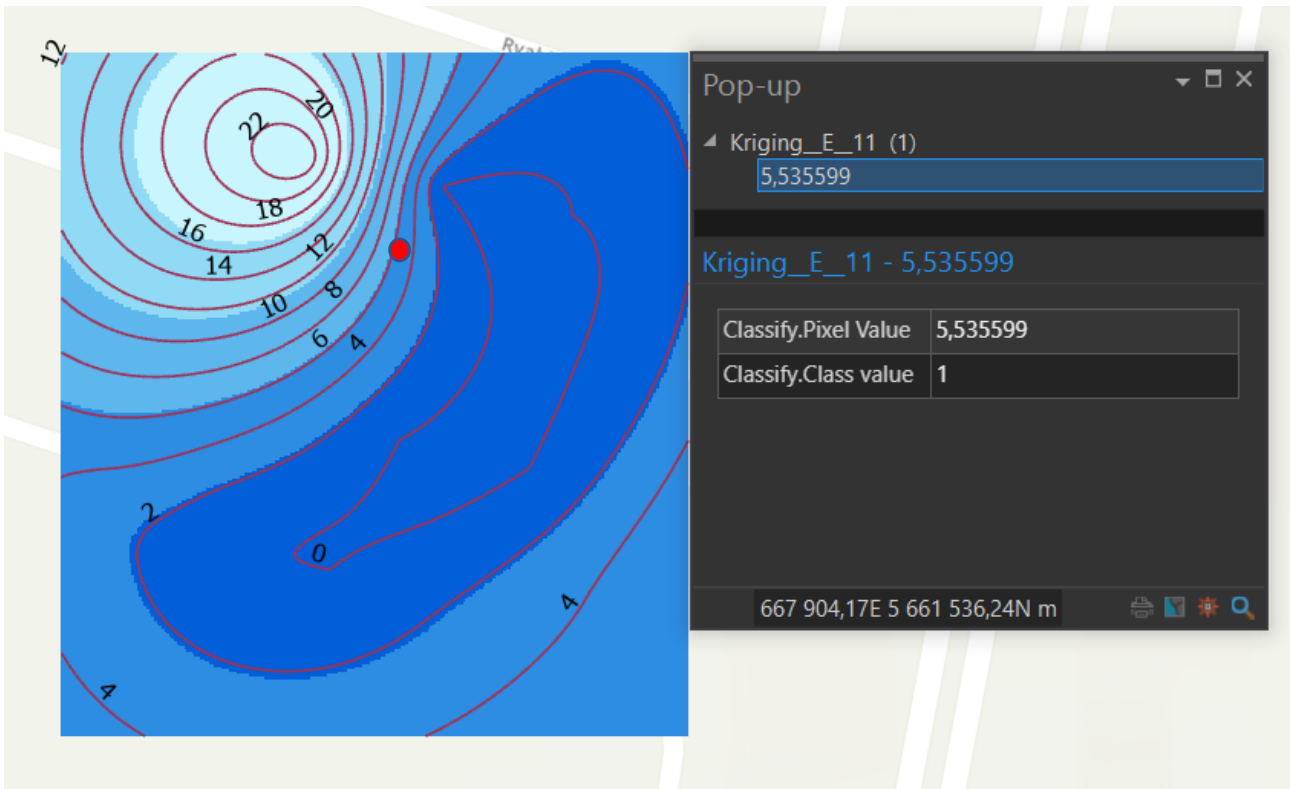


Figure 10 – Raster images of the variability of mechanical characteristics of the soil of the considered territory using the Kriging interpolation method at the depth of 11.5 m

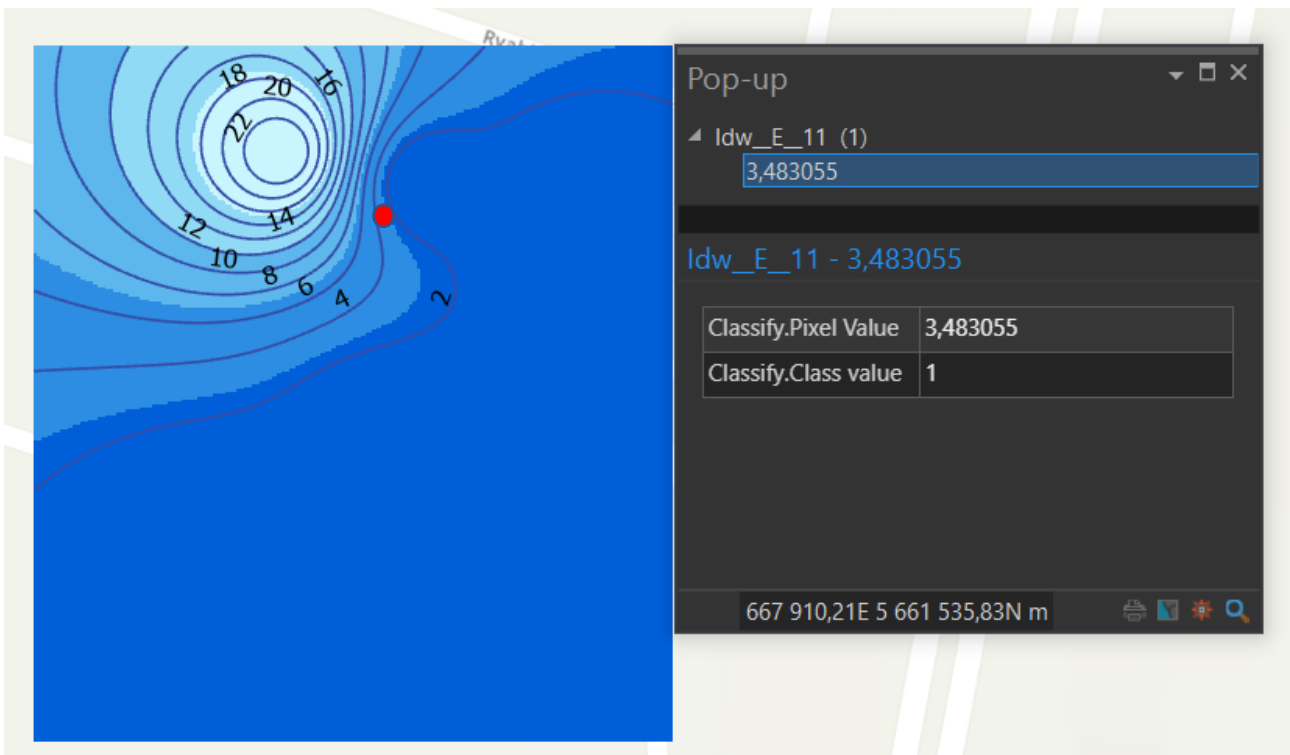


Figure 11 – Raster images of the variability of mechanical characteristics of the soil of the considered territory using the IDW interpolation method at the depth of 11.5 m

Raster images of the variability of soil mechanical characteristics at a depth of 6.5 m show that the strain modulus calculated by the Kriging interpolation method is 8.98, while by the IDW method, it is 6.79. At a depth of 11.5 m, the strain modulus by Kriging is 5.53, while by IDW it is 3.48.

A comparative analysis of the Kriging and IDW methods reveals key differences in their approaches to interpolation and value distribution. Both methods use raw data to produce intermediate values and cover the same number of pixels. However, conceptual differences in their approaches lead to different characteristics of the interpolated surfaces.

The IDW method relies on weighting the values according to the distance to the nearest points. This leads to a more localized distribution of values and consequently to more overlaps and gradations. Visually, this is expressed as undulating shadows and scattered values, reflecting the dependence of the interpolated values on individual points, without taking spatial correlation into account. This approach may not be accurate enough when modeling subsurface spaces, where soil layers typically lie on the same surface and have similar characteristics.

In contrast to IDW, the Kriging method combines the closest points to compute average values, taking into account the spatial correlation between them. This allows for a more correct representation of natural soil variability, especially in complex geologic settings. To demonstrate the effectiveness of Kriging, the pixel distribution was analyzed over a range of values from 15 to 18 (Figures 12 and 13).

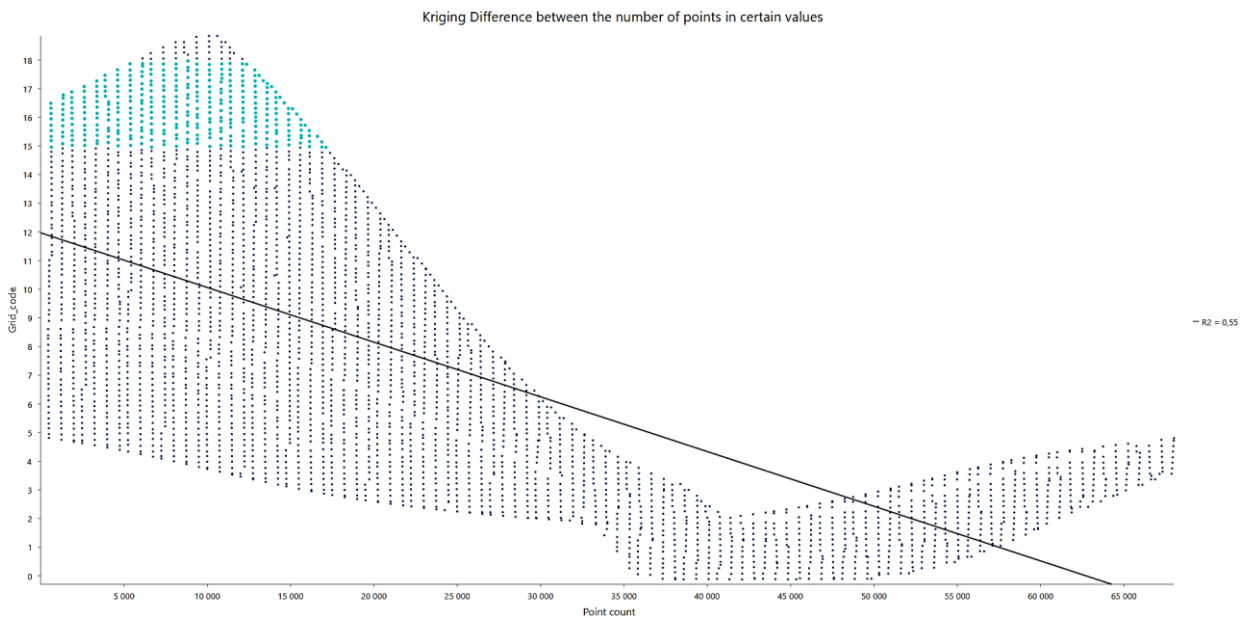


Figure 12 – Difference in the number of points in specified value ranges in Kriging

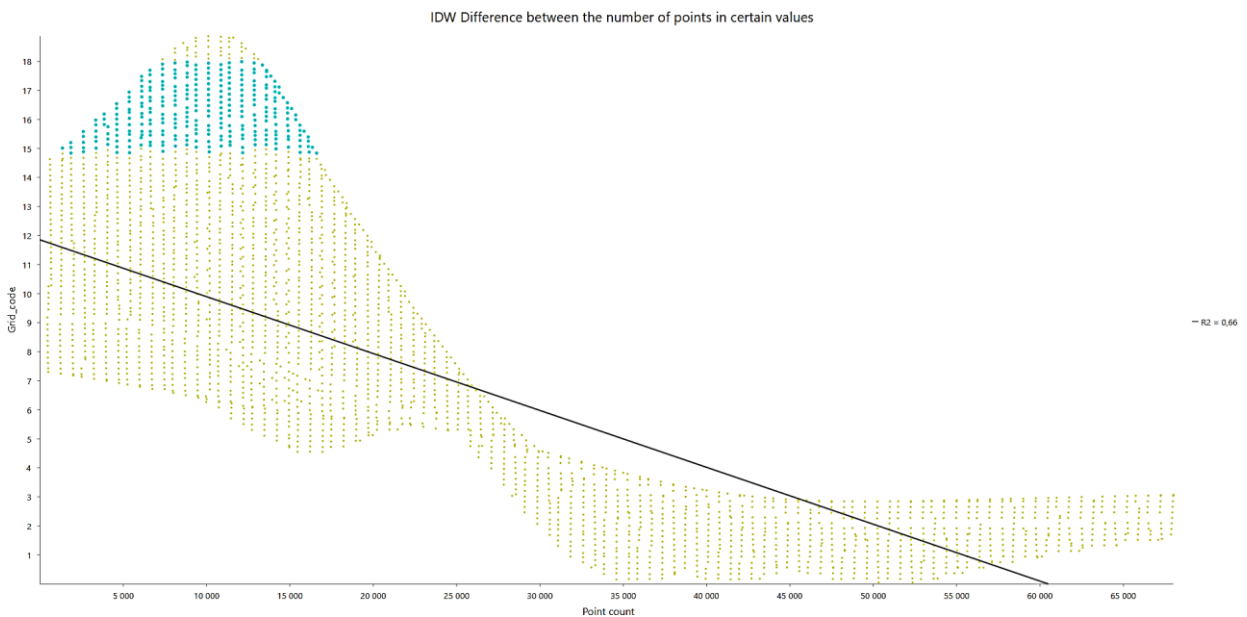


Figure 13 – Difference in the number of points in specified value ranges in IDW

The results showed that IDW covered 2962 pixels whereas Kriging covered 4935 pixels. This confirms that the Kriging method combines similar values more efficiently, increasing the spreading area of the extracted values. Unlike IDW, where the weight of the interpolated values comes from the point itself and results in a more localized distribution, Kriging provides a more uniform distribution of values. This makes Kriging the preferred method for interpolation when accurate modeling of spatial variations and accounting for natural variability in the subsurface is required.

4. Conclusions

This study used ArcGIS to produce detailed raster images of soil properties at depths of 6.5 m and 11.5 m using Kriging and IDW interpolation methods. Kriging provided a wider range of deformation modulus values, from -0.29 to 18.99 MPa at 6.5 m and -0.51 to 23.94 MPa at 11.5 m, capturing greater spatial variability. IDW, with ranges of 3.3 to 18.99 MPa at 6.5 m and 2.6 to 23.99 MPa at 11.5 m, offered localized results based on nearby data points, suitable for more uniform conditions.

Both methods are valuable for geotechnical analysis, with Kriging offering more accurate predictions in areas with complex soil variability, while IDW performs well in data-rich or less variable environments. The choice between methods should be guided by project needs, with both approaches contributing to better design solutions and reduced engineering-geological survey costs.

Acknowledgments

This study was funded by the Committee of Science of the Ministry of Science and Higher Education of the Republic of Kazakhstan (Grant No. AP19676116).

References

- [1] M. I. Wallace and K. C. Ng, "Development and application of underground space use in Hong Kong," *Tunnelling and Underground Space Technology*, vol. 55, pp. 257–279, May 2016, doi: 10.1016/j.tust.2015.11.024.
- [2] I. Vähäaho, "Underground space planning in Helsinki," *Journal of Rock Mechanics and Geotechnical Engineering*, vol. 6, no. 5, pp. 387–398, Oct. 2014, doi: 10.1016/j.jrmge.2014.05.005.
- [3] Y. Li, W. Fan, X. Chen, Y. Liu, and B. Chen, "Safety Criteria and Standards for Bearing Capacity of Foundation," *Math Probl Eng*, vol. 2017, pp. 1–8, 2017, doi: 10.1155/2017/3043571.
- [4] V. N. Bukhartsev and N. T. Pham, "Assessing the Bearing Capacity of Foundation Soul Under Horizontal Load," *Power Technology and Engineering*, vol. 52, no. 4, pp. 413–417, Nov. 2018, doi: 10.1007/s10749-018-0967-4.
- [5] P. V. Loginov, Z. R. Salikhova, and K. S. Sultanov, "Experimental and Theoretical Method for Determining Mechanical Characteristics of Soils under Dynamic Loads," *Mechanics of Solids*, vol. 54, no. 6, pp. 915–928, Nov. 2019, doi: 10.3103/S0025654419060074.
- [6] M. P. Crisp, M. B. Jaksa, and Y. L. Kuo, "Effect of borehole location on pile performance," *Georisk: Assessment and Management of Risk for Engineered Systems and Geohazards*, vol. 16, no. 2, pp. 267–282, Apr. 2022, doi: 10.1080/17499518.2020.1757721.
- [7] W. N. S. Wan-Mohamad and A. N. Abdul-Ghani, "The Use of Geographic Information System (GIS) for Geotechnical Data Processing and Presentation," *Procedia Eng*, vol. 20, pp. 397–406, 2011, doi: 10.1016/j.proeng.2011.11.182.
- [8] A. Antonakos and N. Lambrakis, "Spatial Interpolation for the Distribution of Groundwater Level in an Area of Complex Geology Using Widely Available GIS Tools," *Environmental Processes*, vol. 8, no. 3, pp. 993–1026, Sep. 2021, doi: 10.1007/s40710-021-00529-9.
- [9] P. K. Srivastava, P. C. Pandey, G. P. Petropoulos, N. N. Kourgialas, V. Pandey, and U. Singh, "GIS and Remote Sensing Aided Information for Soil Moisture Estimation: A Comparative Study of Interpolation Techniques," *Resources*, vol. 8, no. 2, p. 70, Apr. 2019, doi: 10.3390/resources8020070.
- [10] P. Singh and P. Verma, "A Comparative Study of Spatial Interpolation Technique (IDW and Kriging) for Determining Groundwater Quality," in *GIS and Geostatistical Techniques for Groundwater Science*, Elsevier, 2019, pp. 43–56. doi: 10.1016/B978-0-12-815413-7.00005-5.
- [11] M. E. M. Jalhoum, M. A. Abdellatif, E. S. Mohamed, D. E. Kucher, and M. Shokr, "Multivariate analysis and GIS approaches for modeling and mapping soil quality and land suitability in arid zones," *Heliyon*, vol. 10, no. 5, p. e27577, Mar. 2024, doi: 10.1016/j.heliyon.2024.e27577.

- [12] T. Fu, H. Gao, and J. Liu, "Comparison of Different Interpolation Methods for Prediction of Soil Salinity in Arid Irrigation Region in Northern China," *Agronomy*, vol. 11, no. 8, p. 1535, Jul. 2021, doi: 10.3390/agronomy11081535.
- [13] J. Zhang, X. Li, R. Yang, Q. Liu, L. Zhao, and B. Dou, "An Extended Kriging Method to Interpolate Near-Surface Soil Moisture Data Measured by Wireless Sensor Networks," *Sensors*, vol. 17, no. 6, p. 1390, Jun. 2017, doi: 10.3390/s17061390.
- [14] Inzhenerno-geologic report, No. 2021-12-IGI-60/ Geocenter Astana LLP. - 2021.
- [15] Mukhamejanova, A., Aldungarova, A., Alibekova, N., Karaulov, S., Kudaibergenov, N., Yespolova, Z., Kurmanova, D., Baizakova, G., & Kazhimkanuly, D. (2024). Toward the use of an intermediate value of the modulus of deformation of soils in geotechnical design. *E3S Web of Conferences*, 559, 01008. doi: 10.1051/e3sconf/202455901008

Information about authors:

Aliya Aldungarova – PhD, Associate Professor, Solid Research Group, LLP, Astana, Kazakhstan; Department of Mining, Construction and Ecology of S. Sadvakasov Agrotechnical Institute of Kokshetau University named after Sh. Ualikhanov, Kokshetau, Kazakhstan, liya_1479@mail.ru

Tymarkul Muzdybayeva – PhD, Senior Lecturer, Department of Civil Engineering, L.N. Gumilyov Eurasian National University, Astana, Kazakhstan, tumar2304@mail.ru

Assel Mukhamejanova – PhD, Acting Associate Professor, Solid Research Group, LLP; Department of Civil Engineering, L.N. Gumilyov Eurasian National University, Astana, Kazakhstan, assel.84@list.ru

Nurgul Alibekova – PhD, Associate Professor, Department of Civil Engineering, L.N. Gumilyov Eurasian National University, Astana, Kazakhstan, nt_alibekova@mail.ru

Khrystyna Moskalova – PhD, Assistant Professor, Senior Research Associate, Department for Research and Development, Development and Training Centre for the Metal Industry, Metal Centre Čakovec, Čakovec, Croatia, krisogasa@gmail.com

Sabit Karaulov – Junior Researcher, Solid Research Group, LLP, Astana, Kazakhstan, karaulovsabit1997@gmail.com

Author Contributions:

Aliya Aldungarova – concept, methodology.

Tumarkul Muzdybayeva – interpretation, drafting.

Assel Mukhamejanova – visualization, editing.

Nurgul Alibekova – resources, data collection.

Khrystyna Moskalova – analysis, testing.

Sabit Karaulov – modeling.

Conflict of Interest: The authors declare no conflict of interest.

Use of Artificial Intelligence (AI): The authors declare that AI was not used.

Received: 22.07.2024

Revised: 11.09.2024

Accepted: 14.09.2024

Published: 15.09.2024



Fractal model of the strength of lightweight concrete based on volcanic tuff taking into account the scale effect

Yerlan Khamza^{1,*}, Vladimir Selyaev², Maratbek Zhuginissov¹, Zhanar Zhumadilova¹

¹Institute of Architecture and Civil Engineering, Satbayev University, 050013, Almaty, Kazakhstan

²Department of Building Structures, Ogarev Mordovia State University, 430005, Saransk, Russia

*Correspondence: y.khamza@satbayev.university

Abstract. The study proposes a fractal model based on B. Mandelbrot's geometry. Mandelbrot geometry to describe the scale effect in concrete. It has been experimentally established that under-loading concrete undergoes degradation of its structure, which is expressed in the sequential destruction of fractals at different scale levels. It was found that the scale reduction leads to an increase in concrete strength: 20x20x20 mm specimens showed the highest strength among all four compositions (23.3-25.3 MPa). The average density of tuff concrete was also investigated: the smallest specimens had a density of 1961.3 kg/m³, while the largest specimens had a density of 1974.2 kg/m³, which is explained by the heterogeneity of the structure and pore distribution. The water permeability of concrete, evaluated through air permeability, showed that specimens with higher air permeability (30.2-30.5 s/cm³) had better water resistance (W14). These data indicate a correlation between air permeability and water resistance, which may be due to the denser structure and improved pore distribution. The study of air permeability makes it possible to predict the durability of concrete structures when exposed to moisture, as well as to improve the quality of building materials and reduce the cost of their operation.

Keywords: fractal dimension, compressive strength, structure, tuff, water permeability.

1. Introduction

When concrete structures (as well as other materials) fail, a characteristic roughness appears on the fracture surface. This relief depends on the material structure, strength ratio, its matrix and grains, loading rate, and other factors that can be observed in the study of different materials. According to the law of similarity, geometrically similar bodies of the same material, made and tested under the same conditions, should have the same strength. This study quantitatively analyzes the fractal and multifractal characteristics of concrete, using the theory of fractal geometry. The study utilizes fractal dimension and multifractal spectrum to describe the defect propagation in concrete. The results show that the fractal dimension effectively estimates the overall defect propagation, with a higher dimension reflecting a greater variety of defects [1].

Concrete, possessing a variety of heterogeneities, has a block-hierarchical structure, which corresponds to the principles of multiscale and self-similarity. Therefore, when describing the degradation process of a concrete structure, it is important to take into account the hierarchically of the block structure and the nesting coefficient of some blocks into others. It is assumed that the contact between the blocks can be represented as dilatant shells, which have different properties from the main body material. Research work [2] covers how the fracture processes in concrete can be analyzed at different scales and supports the view that contacts between structural blocks (dilatant shells) have distinct properties from the bulk material, influencing the material's overall behavior.

Water absorption of concrete is the ability of the material to absorb and retain water that enters it through capillaries and pores. This parameter is an important indicator of concrete quality, as it

directly affects the durability, strength, and resistance of the material to various influences. The water absorption of concrete can affect its properties in the following ways: **Strength:** A high level of water absorption can lead to a reduction in the strength of concrete due to increased porosity and the formation of micro-cracks. **Frost resistance:** Concrete with high water absorption is more susceptible to failure during cyclic freezing and thawing because water freezing in the pores expands and causes mechanical stresses. **Durability:** Increased water absorption favors the penetration of aggressive substances such as chlorides and sulfates, which can lead to corrosion of reinforcement and concrete failure. **Shrinkage and cracking:** Water absorption affects shrinkage processes in concrete, which can lead to cracking and reduced concrete integrity. **Thermal conductivity:** Water in the pores of concrete can alter its thermal conductivity properties, which is important to consider when using the material in different climates. Including water absorption analysis of concrete in the study will allow a more complete assessment of its effect on the fractal dimension of the fracture surface and other key material properties. Relevant data are explored in a paper [3] analyzing the relationship between sorption and capillary coefficients.

However, it has been experimentally found that the strength of geometrically similar specimens depends on their dimensions. This phenomenon is called the scale effect [4], [5]. Several hypotheses have been proposed to explain the nature of the scale effect.

Other studies believe that the manifestation of the scale effect depends on the technology of manufacturing samples of different sizes [6], [7], [8], [9].

Research [10] considers a formalism designed to answer questions about Hamiltonian systems in contact with a thermal bath. The formalism is applied to a simple crack model to find, first, the rate at which a crack moves slowly through a brittle body as a result of thermal fluctuations and, second, the rate at which the crack goes from slow to fast motion. The dominant exponential behavior of these processes is calculated accurately, but the pre-factors are only approximately estimated. Some solutions cannot be considered in the traditional sense as corresponding to a saddle point transition. By considering the crack as an isolated Hamiltonian system, it is shown that irreversible behavior can occur because, although the probability of moving from the past to the present is equal to the probability of moving back from the present to the past, the probability of moving further into the future is exponentially greater.

Research [11] shows that the fractal surface has a multiscale hierarchical structure. In the research, it was found that the structure is preserved when the scale is changed from 0.01 mm to 150 mm. It was obtained that the stress-strain state in the specimen before fracture has little effect on the fractal dimension of the captured periodograms. Their processing showed that the fractal dimension, D , obtained in the splitting experiments ($D=1.061$) and the fractal dimension obtained in the bending experiments ($D=1.057$) are different and on average equal to $D=1.060$. The experiments were carried out on specimens with a cross-section of 100×100 mm in the range of compressive strengths from $R_b=7.5 \div 37.5$ MPa. It was found that the concrete strength does not affect the value of fractal dimension. The values of fractal dimension in the investigated specimens along the crack development and across are practically the same.

In the research [12], the fractal dimensions of the fracture surface of concrete specimens are measured using the periodograms obtained. However, there is no data on the strength of the concrete specimens studied or their composition; the paper does not contain descriptions of the physical and mechanical characteristics of the concrete materials. The only concrete characteristic mentioned in the article is the maximum size of coarse aggregate for each of the tested specimens. As can be seen, in the plastic zone, where different types of fractal-microcracks can be formed from pores and aggregate contacts, they will be partially destroyed along the bonding surfaces when the main crack is formed. When studying the structure of a material that has not yet fractured, the contact zones may be colored by Koch-type curves, which is related to the structure formation process of cement concrete in the process of gaining its ultimate strength.

The study showed [13] that after 28 days of curing, the compressive strength was highest for specimens cured under air conditions ($20 \pm 3^\circ\text{C}$, relative humidity $65 \pm 5\%$) and lowest for specimens cured under conditions ($20 \pm 3^\circ\text{C}$, relative humidity $95 \pm 5\%$). Analyses of the effect of sorption

capacity on compressive strength demonstrated that both surface and internal sorption capacity have no apparent relationship with compressive strength. Although the samples differed in surface water absorption, the difference in internal water absorption was minimal. High surface water absorption reduces the strength of only the surface layer of concrete, while the overall strength of concrete depends on both structures - surface and internal. Consequently, the strength of concrete cannot be evaluated by water absorption alone.

The hypothesis that cement-concrete structures have fractal characteristics has been empirically substantiated. Considering that the concrete structure is subject to process cracks and the possible formation of cracks between aggregate grains, it is logical to use fracture mechanics methods to model the fracture process. The basis of the developed A. Griffith's model is formed on the concepts of Euclidean geometry. It is known that concrete has a fractal structure, which is a concept in the field of geometry. When considering the failure mechanisms of concrete, it is important to consider the invariant multiscale structure of the material. The hypothesis that concrete structure failure can be modeled as a discrete quantum process has been experimentally confirmed [14].

In light of the reviewed literature, the primary issue lies in the incomplete understanding of how concrete's block-hierarchical structure, multiscale behavior, and fractal dimensionality contribute to its fracture processes under varying conditions. While existing studies analyze concrete's structural heterogeneities and the scale effect, the relationship between water absorption and fractal dimensions remains unclear. Additionally, the impact of the scale effect and manufacturing techniques on strength variations across geometrically similar specimens needs further investigation. This gap justifies the study of these factors to improve concrete durability and performance predictions.

The purpose of this article is to investigate the fracture features of concrete structures and to study the influence of various factors on the fractal dimensionality of fracture surfaces. The study analyses geometrically similar concrete specimens, their structure and strength characteristics, and considers the scale effect and its nature. Special attention is given to the block-hierarchical structure of concrete and the principles of multiscale and self-similarity. Additionally, the paper discusses the water absorption of concrete and its effect on the physical and mechanical properties of the material.

2. Methods

2.1 *Materials used in the preparation of the samples*

Filler: Volcanic tuff from the Almaty region of the Republic of Kazakhstan was used as the main concrete filler for the study. Volcanic tuff is a sedimentary rock.

Binder: Portland cement of M500 grade 'Mordovcement PTS 500' of Russian production was used as a binder. Cement "Mordovcement" M500 contains mineral active impurities that determine its properties. It is characterized by the stability of characteristics. It is used in piling foundations, construction of load-bearing structures, and modern highways [15].

Additive: Basalt fiber Cemfibra P was also added to increase the strength. These are fibers that increase the strength of concrete and have a number of advantages over synthetic fibers as they are some of the strongest mineral fibers known to date. Basalt fiber (from roving), is designed for volumetric reinforcement of concrete, mortars, and composite materials. It is used with any dry construction mixtures, as well as concrete for self-mixing [16].

2.2 *Sample Preparation*

After dosage Portland cement and fillers were thoroughly mixed, first in dry form, then water was added, in the amount necessary to obtain a plastic molding mass, water-cement ratio $B/C = 0.6$. To study the properties of the products, standard samples were prepared with dimensions: $20 \times 20 \times 20$ mm and $50 \times 50 \times 50$ mm. The cube specimens were molded on a laboratory vibration platform. The samples were manufactured following the standard [17]. Also, cylindrical specimens of 100 mm diameter were made to determine the water permeability of concrete specimens.

2.3 Determination of the fractal model of concrete strength taking into account the scale effect

The possibility of explaining the scale effect on the basis of the fractal geometry of B. Mandelbrot. It is shown that the main physical essence of the scale effect lies in the scale invariance of the structure at each scale level of the concrete structure. Consequently, the properties appear to be similar. The strength (in kilo-Newtons per square centimeter, megapascals) was determined on cube-shaped specimens with dimensions of 20, 50, and 100 mm. In addition, the discrete, multilevel nature of the failure of concrete specimens with dimensions of 20, 50, and 100 mm was confirmed by the strain diagram obtained on a Wille Geotechnik testing machine (model 13-PD/104). The tests were carried out at a loading rate of 0.5 mm/min with readings recorded at a rate of 10 measurements per second. Compositions N2, N5, N17, N18 were produced. For each composition, there were 9 cube samples with rib sizes of 20, 50, and 100 mm. In Figure 1, we can observe the failure process of the samples. The strength values were also determined by standard [17].



a) Strength test of the specimen with dimensions 20×20×20 mm



b) Strength test of the specimen with dimensions 50×50×50 mm

Figure 1 – The failure process of the samples

2.4 Determination of average density

The following method was used to determine the average density of tuff concrete samples by standard [18]. For regular cubes, volume measurement was carried out using measuring tools such as a ruler and caliper, with an allowable error of no more than 1 mm. For non-uniform samples, it was recommended to use the hydrostatic method for mass determination or the volumetric method for volume measurement based on weighing.

2.5 Determination of water absorption

The AGAMA-2PM instrument was installed on the surface of the tested product using sealing mastic (Figure 2) in accordance with standard [19]. Then the piston in the chamber of the device was moved to create rarefaction, which was recorded by the pressure sensor. According to the change in pressure, the resistance of the material to air penetration was determined. The test was carried out at air temperature up to 26°C. The vacuum pressure in the chamber of the device was maintained at a minimum of 0.06 MPa. No more than 300 N of force was required to create a working vacuum in the chamber. The range of measurements included material resistance to air penetration from 0.1 to 999.9 s/cm³ and concrete water resistance grades from 0 to 20. The tolerance limit of relative error of resistance determination did not exceed 8%.



Figure 2 – Determination of water absorption on the AGAMA-2RM device

3. Results and Discussion

3.1 Determination of a fractal model of concrete strength taking into account the scale effect

The analysis confirms the multifractality and self-similarity of concrete structure as an objective manifestation of material properties that can be quantified using the fractal dimension. The graphs presented (Figure 3) demonstrate that the failure of the specimen structure is gradual rather than instantaneous. The peaks denoting the moment of fracture have an enlarged shape, showing both an increase and decrease in amplitude. However, the graph shows an oscillatory pattern as the structure gradually collapses.

Figure 3 is four enlarged sections of the same graph. The figure shows the fracture graph of 50x50x50 mm specimens of N5 composition.

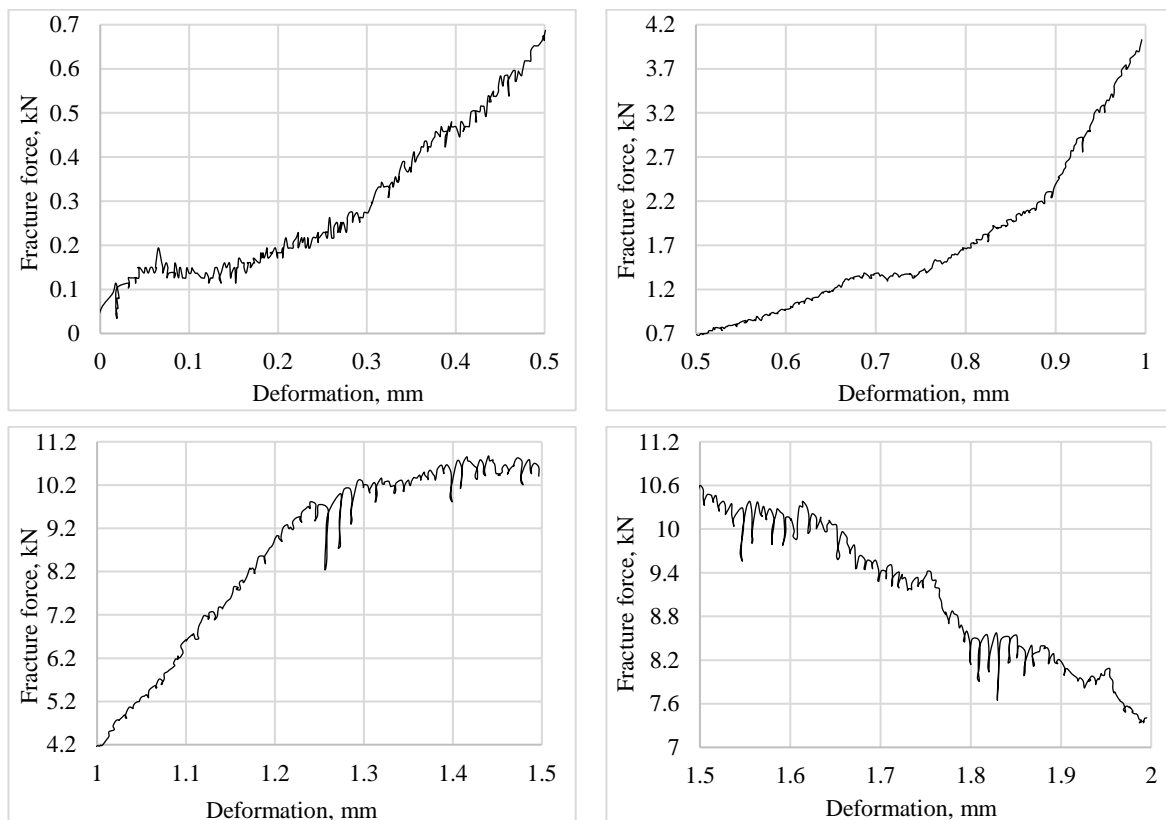


Figure 3 – Extended strain zones of a 50x50x50 mm specimen ranging from 0 mm to 2.0 mm

Table 1 shows the values after testing the specimens with the same composition at the age of 7 days. We can observe the influence of scale effect on the properties of tuff concrete depending on the size of the specimens.

Table 1 – Strength and density indices of samples depending on their size

No	20x20x20, MPa	50x50x50, MPa	100x100x100, MPa	Average density, kg/m ³
N2	23.3	21.7	20.0	1961.3
N5	22.8	22.4	20.3	1851.2
N17	25.3	24.1	23.6	2085.6
N18	24.9	22.4	22.2	2128.5

Concrete consists of various components such as cement, aggregates, and reinforcing materials. Various stresses and loads can cause the bonds between these components to break, resulting in the failure of the concrete structure. The concrete matrix is a bonding material containing reinforcing materials. Exposure to load can cause failure and cracking of the concrete matrix. In Figure 4, we can observe the changes in the strength plot as a function of specimen size. We can see that in all compositions, the specimen strength increases with decreasing specimen size.

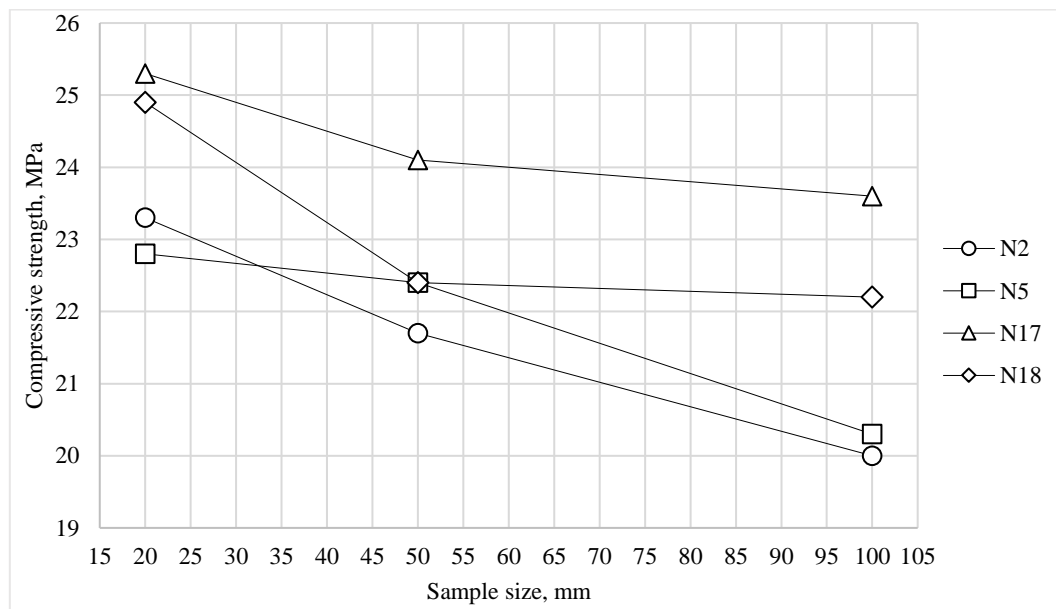


Figure 4 – Strength values of specimens depending on their size

Investigations of the compressive strength values of tuff concrete specimens of different sizes revealed a significant influence of the scale effect on the mechanical properties of the material. In particular, the 20x20x20 mm specimens showed the highest compressive strength in all four compositions, which is noticeably higher than that of larger specimens. This phenomenon is explained by the fact that smaller specimens have fewer defects and cracks, which contributes to higher strength. This supports the hypothesis of the fractal structure of concrete, where a decrease in scale leads to an increase in the strength of the material. Such results are important for the practical application of tuff concrete as they indicate the need to consider specimen size in structural design and testing.

The assumption of fractal structure of cement concrete with volcanic tuff is experimentally substantiated. The mechanism of concrete failure taking into account the invariant multifractal structure is considered. The discrete fracture process of concrete structures is experimentally confirmed. Depending on the size of tuff concrete specimens, different strength values were obtained for the same composition. The smallest size specimens showed higher strength even considering the correction factor. From the test results, an increase in strength was observed for specimens with 20 mm faces in contrast to specimens with faces of 50 and 100 mm.

3.2 Determination of average density

Measurements of the average density of tuff concrete samples of different sizes also showed interesting results. The smallest samples of size 20x20x20 mm had an average density of 1961.3 kg/m³, which was slightly higher than the average size 50x50x50 mm samples which had a density of 1958.4 kg/m³. The largest 100x100x100 mm specimens showed the highest density of 1974.2 kg/m³. The differences in density can be explained by the heterogeneity of the structure and the distribution of pores and voids in the material. The larger samples have a larger volume, which may contribute to a more uniform distribution of voids and hence a higher density. These findings emphasize the importance of careful control of density parameters in the production and application of tuff concrete, as they significantly affect the strength characteristics and durability of the final structures.

3.3 Determination of water absorption.

To determine the water permeability of concrete, the 'air permeability' method was used using the AGAMA-2RM device. Unlike the 'wet spot' method, this method does not disturb the structure of the sample.

The principle of operation of the AGAMA-2PM device is to measure the pressure in a sealed chamber where a rarefaction is created. This rarefaction increases due to the penetration of atmospheric air through pores and defects of the sample. The device provides a hermetic connection to the surface of the material through a special mastic.

The waterproofness grade of concrete (W) is determined based on the calculated parameters a and m - the resistance of the material. To obtain the result of air permeability tests, the arithmetic mean value of the air resistance of concrete measured on a set of six specimens was used.

Table 2 shows the results of the tests carried out using the AGAMA-2PM instrument.

Table 2 – Water permeability values of samples

No	Air resistance of concrete, s/cm ³	Water resistance, MPa	Waterproof grade, W
N2	28.1	1.2	W12
N5	28.5	1.2	W12
N17	30.2	1.4	W14
N18	30.5	1.4	W14

The study of the water permeability of concrete based on its air permeability values is of considerable interest to modern construction technology. In the data presented, concrete grades N2, N5, N17, and N18 showed different levels of air permeability and thus water resistance. Specifically, specimens N2 and N5 have an air permeability of 28.1 and 28.5 s/cm³, respectively, and water resistance of 1.2 MPa, corresponding to water resistance class W12. On the other hand, samples N17 and N18 showed higher air permeability of 30.2 and 30.5 s/cm³, respectively, and water resistance of 1.4 MPa corresponding to water resistance class W14. These data suggest that higher air permeability correlates with higher water resistance, which may be due to the denser concrete structure and improved pore distribution.

The study [20] assesses the quality of the concrete protective layer, which is necessary for the proper maintenance of concrete structures. Concrete strength is assessed mainly by chloride penetration, neutralization and other external factors. The authors analyze the relationship between concrete air permeability and its durability indicators, such as chloride diffusion and neutralization, and propose using air permeability as an indicator of concrete durability. Experiments have shown a high correlation between air permeability, neutralization and diffusion coefficients of chlorine ions. Another study [21] also presented a method for measuring concrete permeability using the flow pump technique previously used to assess soil permeability. A new simple method for determining permeability was also proposed, based on a modification of the Valenta formula taking into account the apparent air content in concrete mixtures. Four types of concrete were studied: without additives,

with an admixture to increase strength, with a superplasticizer, and with both additives simultaneously. The results showed that the proposed method provides reliable measurements in a short period of time and can be useful in engineering practice for hydraulic concrete structures, bridges, underground parts of buildings, and sealed tanks.

4. Conclusions

The study confirmed the multifractality and self-similarity of concrete structures, as evidenced by the fractal dimension. The failure of the specimens was gradual, with an oscillatory pattern in the graphs, indicating a progressive collapse rather than an instantaneous fracture.

The 20x20x20 mm specimens demonstrated the highest compressive strength: N2 with 23.3 MPa, N5 with 22.8 MPa, N17 with 25.3 MPa, and N18 with 24.9 MPa. This supports the hypothesis that smaller scales enhance material strength due to the fractal nature of the concrete.

In terms of density, the 20x20x20 mm specimens had an average density of 1961.3 kg/m³, slightly higher than the 50x50x50 mm specimens at 1958.4 kg/m³. The largest 100x100x100 mm specimens had the highest density at 1974.2 kg/m³, likely due to more uniform pore distribution.

Water permeability, inferred from air permeability measurements, showed that specimens N2 and N5, with air permeabilities of 28.1 and 28.5 s/cm³ respectively, had water resistances of 1.2 MPa (W12). In contrast, specimens N17 and N18 had higher air permeabilities of 30.2 and 30.5 s/cm³ and water resistances of 1.4 MPa (W14). This suggests that increased air permeability correlates with higher water resistance, possibly due to a denser concrete structure.

Overall, the study indicates that air permeability can reliably predict water resistance, contributing to the development of more durable and cost-effective concrete formulations. Future research could further refine these relationships to advance construction materials and practices.

Acknowledgments

The authors would like to acknowledge that this work was carried out in the laboratories of the Ogarev Mordovia State University and Satbayev University. Their support and resources were invaluable in conducting this research.

References

- [1] J. Shen, Q. Xu, and M. Liu, "Fractal Analysis of Defects in Concrete under Elevated Temperatures," *ACI Mater J*, vol. 8, no. 6, p. 304, May 2022, doi: 10.14359/51737183.
- [2] J. G. M. van Mier, *Fracture Processes of Concrete: Assessment of Material Parameters for Fracture Models*. Boca Raton: CRC Press, 2017. doi: 10.1201/b22384.
- [3] J. Gong, W. Zhang, and Z. Zhou, "Foam Concrete Pore Structure Effect on Drying Shrinkage and Frost Resistance," *J Test Eval*, vol. 49, no. 5, pp. 3431–3443, Sep. 2021, doi: 10.1520/JTE20190550.
- [4] J. Su and Z. Fang, "Scale effect on cubic compressive strength of ordinary concrete and high-strength concrete," *Jianzhu Cailiao Xuebao/Journal of Building Materials*, vol. 16, pp. 1078-1081+1086, Sep. 2013, doi: 10.3969/j.issn.1007-9629.2013.06.028.
- [5] J. Zhuo, Y. Zhang, M. Ma, Y. Zhang, and Y. Zheng, "Uniaxial Compression Failure and Size Effect of Recycled Aggregate Concrete Based on Meso-Simulation Analysis," *Materials*, vol. 15, no. 16, p. 5710, Aug. 2022, doi: 10.3390/ma15165710.
- [6] N. Zabihi, "Effect of Specimen Size and Shape on Strength of Concrete," Eastern Mediterranean University, Gazimağusa, North Cyprus, 2012. doi: 10.13140/RG.2.2.17927.83360.
- [7] S. Issa, M. Islam, M. Issa, A. Yousif, and M. Issa, "Specimen and Aggregate Size Effect on Concrete Compressive Strength," *Cement, Concrete, and Aggregates*, vol. 22, no. 2, pp. 103–115, Dec. 2000, doi: 10.1520/CCA10470J.
- [8] X. Li *et al.*, "Study on the Influence of Specimen Size and Aggregate Size on the Compressive Strength of Rock-Filled Concrete," *Applied Sciences*, vol. 13, no. 10, p. 6246, May 2023, doi: 10.3390/app13106246.
- [9] J.-I. Sim, K.-H. Yang, H.-Y. Kim, and B.-J. Choi, "Size and shape effects on compressive strength of lightweight concrete," *Constr Build Mater*, vol. 38, pp. 854–864, Jan. 2013, doi: 10.1016/j.conbuildmat.2012.09.073.
- [10] M. Marder, "Statistical mechanics of cracks," *Phys Rev E*, vol. 54, no. 4, pp. 3442–3454, Oct. 1996, doi: 10.1103/PhysRevE.54.3442.

- [11] I. G. Shapiro, G. A. Shapiro, and B. A. Loginov, "To the question of fractography of concrete," *Construction and Reconstruction*, vol. 77, no. 3, pp. 31–38, 2018.
- [12] V. E. Saouma, C. C. Barton, and N. A. Gamaleldin, "Fractal characterization of fracture surfaces in concrete," *Eng Fract Mech*, vol. 35, no. 1–3, pp. 47–53, Jan. 1990, doi: 10.1016/0013-7944(90)90182-G.
- [13] S. P. Zhang and L. Zong, "Evaluation of Relationship between Water Absorption and Durability of Concrete Materials," *Advances in Materials Science and Engineering*, vol. 2014, pp. 1–8, 2014, doi: 10.1155/2014/650373.
- [14] V. P. SEL'YAEV, P. V. SEL'YAEV, S. Y. GRYAZNOV, and M. Y. AVERKINA, "STRENGTH AND FRACTURE MECHANICS OF THE FRACTAL STRUCTURE OF CONCRETE," *Expert: Theory and Practice*, vol. 20, no. 1, pp. 35–43, 2023, doi: 10.51608/26867818_2023_1_35.
- [15] "Cement Mordovcement M500 D20 meshok 50kg." Accessed: Sep. 15, 2024. [Online]. Available: <http://spectorg-cement.ru/product/pts-m500-d20-mordovtsement>
- [16] "Fibra bazaltovaya CemFibra R 1 kg." Accessed: Sep. 15, 2024. [Online]. Available: <https://leroymerlin.kz/product/fibra-bazaltovaya-cemfibra-r-1-kg-82553541/#params>
- [17] *GOST 10180-2012 Concretes. Methods for strength determination using reference specimens*. 2012.
- [18] *GOST 12730.1-78 Concretes. Methods of determination of density*. 1978.
- [19] *GOST 12730.5-2018 Concretes. Methods for determination of water tightness*. 2018.
- [20] D. N. Katpady, H. Hazehara, M. Soeda, T. Kubota, and S. Murakami, "Durability Assessment of Blended Concrete by Air Permeability," *Int J Concr Struct Mater*, vol. 12, no. 1, p. 30, Dec. 2018, doi: 10.1186/s40069-018-0260-9.
- [21] Z. Skutnik, M. Sobolewski, and E. Koda, "An Experimental Assessment of the Water Permeability of Concrete with a Superplasticizer and Admixtures," *Materials*, vol. 13, no. 24, p. 5624, Dec. 2020, doi: 10.3390/ma13245624.

Information about authors:

Yerlan Khamza – Master of Engineering Sciences, Head of the Laboratory, Institute of Architecture and Civil Engineering, Satbayev University, 050013, Almaty, Kazakhstan, y.khamza@satbayev.university

Vladimir Selyaev – Doctor of Technical Sciences, Professor, Head of Department, Department of Building Structures, Ogarev Mordovia State University, ntorm80@maul.ru

Maratbek Zhuginissov – Doctor of Technical Sciences, Professor, Lecturer, Institute of Architecture and Civil Engineering, Satbayev University, 050013, Almaty, Kazakhstan, m.zhuginissov@satbayev.university

Zhanar Zhumadilova – PhD, Associate Professor, Vice Director, Institute of Architecture and Civil Engineering, Satbayev University, 050013, Almaty, Kazakhstan, z.zhumadilova@satbayev.university

Author Contributions:

Yerlan Khamza – concept, methodology, resources, data collection, testing, modeling, funding acquisition.

Vladimir Selyaev – concept, analysis, visualization.

Maratbek Zhuginissov – methodology, interpretation, drafting.

Zhanar Zhumadilova – analysis, visualization, interpretation, drafting, editing.

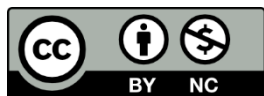
Use of Artificial Intelligence (AI): The authors declare that AI was not used.

Received: 29.07.2024

Revised: 14.09.2024

Accepted: 15.09.2024

Published: 16.09.2024



Copyright: © 2024 by the authors. Licensee Technobius, LLP, Astana, Republic of Kazakhstan. This article is an open access article distributed under the terms and conditions of the Creative Commons Attribution (CC BY-NC 4.0) license (<https://creativecommons.org/licenses/by-nc/4.0/>).



Binding properties of synthesized CS glasses activated by alkaline components

 Bakhytzhan Sarsenbayev¹,  Sultan Auyesbek^{1,*},  Meiram Begentayev²,
 Nuraly Sarsenbayev¹,  Erkin Khaltursunov³,  Gaukhar Sauganova¹

¹M. Auezov South Kazakhstan University, Shymkent, Kazakhstan

²Kazakh National Research Technical University named after K. Satpayev, Almaty, Kazakhstan

³Turin Polytechnic University in Tashkent, Tashkent, Uzbekistan

*Correspondence: sultan_067@mail.ru

Abstract. The paper presents the synthesis and evaluation of hydration and binding properties of individual minerals with glass-like structures in silicate systems, most often found in technogenic materials based on phosphorus and blast furnace slags. This work aims to determine the optimum composition of CS glasses to obtain binders with given properties, the hydration of glasses of different silicate and aluminosilicate compositions in the presence of solutions of soda, sodium hydroxide, and sodium metasilicate was investigated. The results of X-ray phase and differential-thermal analysis, and infrared spectrum are given, and the hydration structure of the calcium oxide-silicon oxide-alkali component system has been studied. The analysis of hydrate neoplasms of the studied binding systems shows that the most optimal conditions for the synthesis of stone strength with stable physical and mechanical properties are created in the presence of gel-like phase reinforced by hydrosilicates and hydroaluminosilicates of alkaline and alkaline-alkaline-earth composition, characterized by fiber-like structure and possessing the ability to epitaxial fusion with each other, as well as gel-like phase, which they reinforce.

Keywords: low basic tobermorite-like hydrosilicates, heat and humidity treatment, alkaline components, differential thermal analysis, slag-alkali binders, hydration.

1. Introduction

The study of properties of individual glasses and minerals included in blast furnaces and phosphorus slags has been studied by many researchers: Lanzhvan S., Keil F., Lapin V.V., Butt Yu.M., and many others. However, the author and his collaborators conducted the most successful research in synthesized glasses and minerals [1], [2].

In [3] the results of studies of the hydraulic activity of one-calcium silicate (CaOSiO_2) and gelenite ($2\text{CaOAl}_2\text{O}_3\text{SiO}_2$) were published. Testing of samples of $7\times 7\times 7$ cm with and without the addition of activating components was carried out after storage in water for 28 days, steaming according to the regime of 4+8+2 h and autoclave treatment for 4 h at 0.8 MPa. Analyzing the data, it is possible to draw a conclusion that slowly cooled minerals do not possess binding properties. However, at their activation with lime, lime in combination with gypsum and Portland cement clinker the hydraulic activity of CS and C_2AS slightly increases.

Researchers [4] found that the reactivity of glasses mainly depends on the CaO content because calcium depolymerizes the glass structure and increases the reaction rate of glasses. The reactivity of glasses is mainly related to the degree of depolymerization of the glass structure. In this work, eight calcium aluminosilicate glasses have been synthesized, whose compositions reflect the glassy phases of industrial ashes and slags. The selected composition ranges allow the roles of Ca and Al to be distinguished and identified. The effect of Al_2O_3 on the reactivity of the glass is less pronounced and is based on the chemical weakening of the glass structure. However, an increase in

alumina content has a pronounced effect on hydrate phase assembly, bound water content, portlandite consumption, and heat of reaction. The compressive strength of composite cement mortars incorporating synthesized CaO-Al₂O₃-SiO₂ glasses was found to depend on both the degree of reaction of the glass and the actual composition of the phases.

In [5] the influence of vanadium oxide on the crystallization of CaO-Al₂O₃-SiO₂ (CAS) glass was studied. Specifically, CAS glass-ceramics with deposited hexagonal lamellar particles of metastable CaAl₂Si₂O₈ (CASGC-H), which is a layered crystal that was prepared using metallic molybdenum (Mo) particles as a nucleation agent, was investigated. When the parent CAS GC-H glass was crystallized with the addition of vanadium oxide in the range of 0.052-0.21 weight %, the resulting lamellar particles of metastable CaAl₂Si₂O₈ showed an increase in aspect ratio from 20 to 15 compared to conventional CAS GC-H.

Furthermore, no crystallization occurred in CAS glass with vanadium oxide in the range of 0.052-0.21 wt% in the absence of metallic Mo particles. At the same time, in CAS glass containing 1.0 wt% vanadium oxide without the addition of Mo metal particles, the precipitation of metastable CaAl₂Si₂O₈ was observed. Thus, these results indicated that the aspect ratio of layered crystals in the glass is controlled by the addition of a relatively small amount of vanadium oxide, and a new nucleator was developed for the deposition of metastable CaAl₂Si₂O₈ in CAS glass using a relatively high vanadium oxide content.

The authors [6] carried out microstructural control of CaO-Al₂O₃-SiO₂ (CAS) glass-ceramics which was achieved by oxidation and mixing with nucleating agents. The CAS glass-ceramics were deposited with hexagonal lamellar particles of metastable layered CaAl₂Si₂O₈ (CAS GC-H) crystals, which are usually prepared in a reducing atmosphere forming metallic Mo or W particles as nucleating agents.

The average crystal particle size decreased significantly from 50 to 11 μm when CAS GC-H containing metallic W particles was prepared in an oxidizing atmosphere. Compared with this CAS-GC-H, the crystal particle size increased from 8-20 to 10-30 μm when CAS GC-H was prepared by mixing the glass mass containing metallic Mo and the glass mass containing metallic W particles. These results indicate that the microstructure of CAS GC-H is controlled on a micrometer scale from the parent glass with the same composition by varying the experimental conditions related to the melting state of the glass.

According to the author [7], hydration and hardening of unfired slag binders occur through the formation of silicic acid, which further interacts with calcium hydroxide. This physicochemical process results in the formation of calcium hydrosilicates in gel, subcrystalline, and crystalline forms. As they accumulate, these new formations bind together the particles of the hardening system, which, thickening over time, acquires density and strength.

The closest to our ideas about the mechanism of hydration and hardening of slag-alkali binders are the authors of works [8], so further we consider his vision of this mechanism. Processes of hydration of slag-alkali binders develop differently depending on the type of slag and alkaline component of curing systems.

Irrespective of the ways of their development, it is unrealistic to realize hydration only through the dissolution of slag-alkali binder components. In hydration processes occurring in solidifying slag-alkali systems, the formation of hydrogels, rather than the dissolution of silicate components, plays a decisive role.

It follows that the synthesis and evaluation of hydration and binding properties of blast-furnace and phosphorus slag constituents and the development of binding materials on their basis is an urgent problem.

The goal of current research is to investigate and determine the optimum composition of CS glasses for obtaining binders with given properties hydration of glasses of different silicate and aluminosilicate compositions in the presence of solutions of soda, sodium hydroxide, and sodium metasilicate.

2. Methods

Synthesized glasses were obtained by abrupt cooling of melts of the corresponding chemical composition, which were ground in porcelain mills to a specific surface of $350\text{m}^2/\text{kg}$. The materials thus obtained were grouted with solutions of soda, caustic soda, and liquid glass. The test specimens with the size of $1\times 1\times 1$ cm from a dough of normal density were hardened in natural conditions, in water, and hydrothermal conditions at temperatures of 95 and 175°C under the regime of 1.5+2+4+2 h.

Natural and water-cured specimens were tested after 3, 28, 90, and 360 days, and steamed and autoclaved specimens 24 hours after hydrothermal treatment.

X-ray phase analysis was carried out on a diffractometer URS 50 IM and DRON-3M in the range of angles $2\theta = 10\dots 60^\circ$ at a counter and sample rotation speed of 2° per minute. The decoding of X-ray radiograms was carried out by identification of the obtained data with the characteristics of natural and artificial minerals. DTG, DTA, and TG curves were recorded on a derivatograph of the Paulik R. and Erden L. system of the MOM Budapest company. Spectral analysis was carried out on a Specord-80

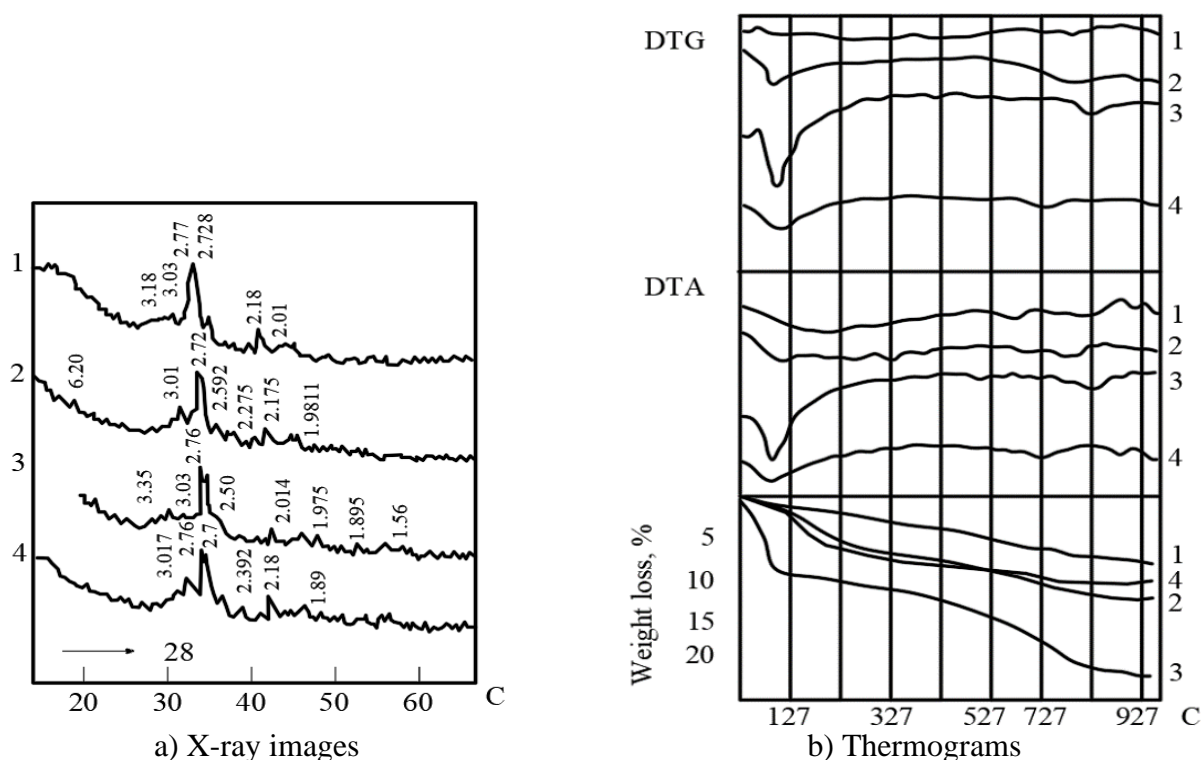
3. Results and Discussion

3.1 Calcium oxide-silicon oxide-alkali component system $3\text{CaO}\cdot 2\text{SiO}_2(\text{C}_3\text{S}_2)$

During the hydration of pure C_3S_2 in water, the formation of weakly crystallized low basic hydrosilicates like tobermorite 11,3A and insignificant amounts of afvillite is observed.

When gelled with NaOH and Na_2SiO_3 solutions, the composition of hydration products is represented by afvillite CSH(1), plombierite and sodium-calcium compound $\text{NaCa}_2\text{Si}_3\text{O}_8\text{OH}_2\text{Na}_8\text{Ca}_8\text{Si}_5\text{O}_{26}\text{H}_{14}$ ($d/n = 3.09; 2.26$ and 2.01 Å) of cryptocrystalline structure (Figure 1a).

On IR spectrograms the presence of lines at 3340, 1658, 1280, 1100, 883, 673, and 512 cm^{-1} (Figure 1c) is identified with absorption lines characteristic of afvillite, and the formation of low-base hydrate phases is confirmed by the shift of absorption bands at 1000, 1070 cm^{-1} to lower frequencies due to polycondensation of silicon-oxygen groups.



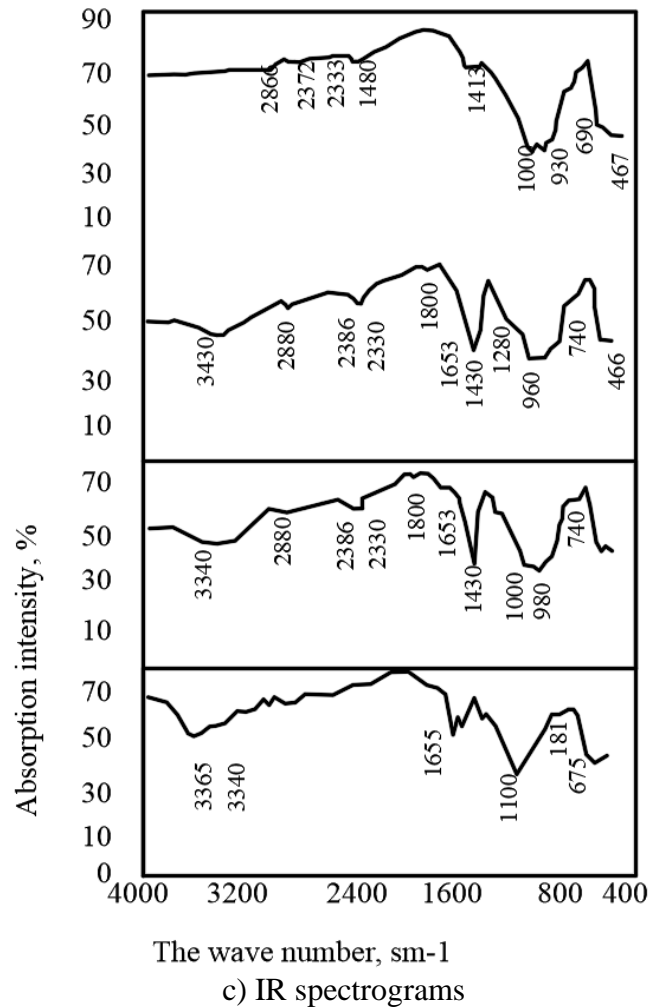


Figure 1 – Results of the analysis of a stone based on a glass-like analog of C_3S_2

On DTA according to Figure 1(b), the presence of endothermic effects at 240, 320, 520, and 800 °C is due to stepwise dehydration, and endothermic effects at 100, 130 °C and exo-effect at 850 °C tobermorite dehydration and α -CS crystallization. The phase composition of the firing products of the composition based on C_3S_2 and NaOH according to Figure 2.2 is represented by β - C_2S and $Na_2O \cdot CaO \cdot SiO_2$, and the composition based on C_3S_2 , $Na_2O \cdot SiO_3$ - β -CS, C_3S_2 and an insignificant amount of α -CS (Figure 2).

Comparison of phase compositions of hydration and dehydration products of glass-like C_3S_2 hydrated with NaOH and Na_2SiO_3 solutions shows that in the first case, more intensive destruction of glassy substance and formation of more mixed sodium-calcium compounds are observed, while at the hydration of C_3S_2 in the presence of Na_2SiO_3 afvillite and low-basic tobermorite-like hydrosilicates with inclusions of alkali ions are formed.

After heat and humidity treatment, the phase composition of hydration products of glass-like C_3S_2 in the presence of NaOH and Na_2SiO_3 along with compounds formed during curing under normal conditions in accordance with Figure 3 includes low-basic hydrosilicates of scautite type ($d/n=3.03$; 2,78; 2,39 and 2,29 Å), and transformations of calcium hydrosilicates within isomorphous phases (CSH(I)→scoutite) almost does not affect physical and mechanical properties of dispersed structures, as the new phase forms good contacts of aggregation with the disappearing one.

On the DTA curve according to Figure 1b the formation of $C_3S_2H_3$ is confirmed by the presence of endo-effect at 360...400 °C and exo-effect at 780 °C, the shift of which in the low-temperature region is due to the presence of Na^+ ions, and the synthesis of tobermorite-like calcium

hydrosilicates by the presence of endo-effects at 90...220 °C, 300...340 °C and exo-effect at 900 °C, associated with the crystallization of β - C₃S.

The formation of sodium-calcium compounds during hydration of C₃S₂ with NaOH solution under conditions of heat and humidity treatment is confirmed by the presence of endo effects at 540-550-600 °C on the DTA curve.

At mixing of glass-like C₃S₂ with NaCO₃ solution in the composition of hydration products (after the heat and humidity treatment) in addition to compounds formed at hydration in the presence of NaOH - a phase of pyrsonite type Na₂Ca(CO₃)₂·25H₂O was identified, the formation of which is confirmed by the presence of endothermic effect at 760 °C on the DTA-curve in accordance with Figure 3b.

3.2 The system of CaO-SiO₂(CS)

During hydration of the glass-like analog under normal conditions, the degree of hydrolytic degradation is insignificant.

After heat and humidity treatment the composition of hydrate neoplasms is represented by C₃S₂H₃ and partially crystallized tobermorite-to-like calcium hydrosilicates, the formation of which is confirmed by the presence on the DTA-curve of endothermic effects at 240 ... 260, 320, 470 °C (dehydration of C₃S₂H₃), endo effect at 240 °C and exo effect at 880...960 °C (dehydration of low-base calcium hydrosilicates).

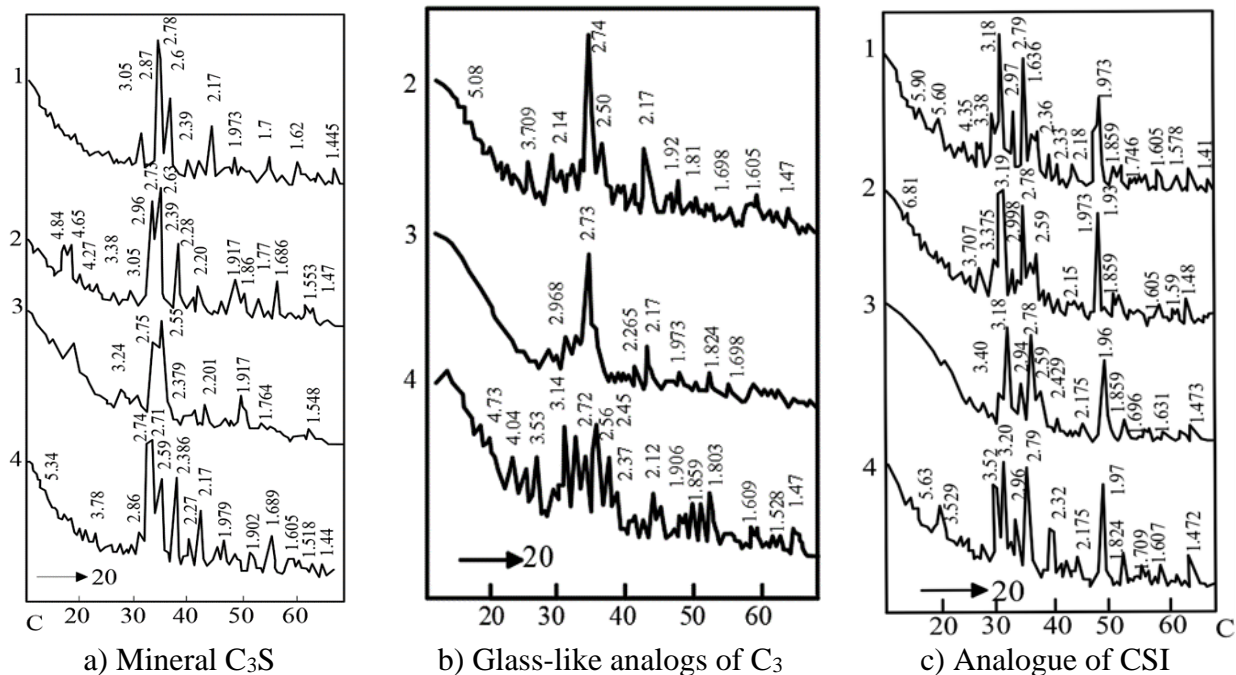


Figure 2 – X-ray images of a stone dehydrated at N = 1000 °C: 1 – water; 2 – solution NaOH; 3 – solution Na₂CO₃; 4 – solution Na₂SiO₃

During hydration of the glass-like analog of CS in the presence of NaOH, the phase composition of neoplasms after 28 days of hardening in accordance with Figure 4a is represented by low-base phases of the cryptocrystalline structure: gyrolite (d/n = 3.36; 3.15; 3.02; 2.52; 2.25 Å) and pectolite.

On the DTA curve, in accordance with Figure 4 (b), the appearance of endothermic effects at 140...180 °C, 500...780 °C, and the exo-effect at 820 °C is due to dehydration of gyrolite, and the exo-effect at 860...880 °C is due to dehydration of CSH(I) and crystallization of β -CS. The displacement of the exo-effect to the region of elevated temperatures is explained by the high content of calcium in the composition of the hydrosilicate phases.

The shaft of the eco effect to the region of elevated temperature is explained by the high content of calcium in the composition of the hydrosilicate phases.

After heat and moisture treatment at $T=100\text{ }^{\circ}\text{C}$, the presence of $\text{C}_6\text{S}_6\text{H}$ (d/n) carbonatite was noted in the phase composition of hydration products along with CSH(I) and tobermorite = 3.23; 3.0; 2.83; 2.72; 2.51 and 2.04 \AA (Figure 3d).

The formation of low-basic tobermorite-like phases is confirmed by the presence on the DTA curve of endothermic effects at $90 \dots 120\text{ }^{\circ}\text{C}$, $300 \dots 340\text{ }^{\circ}\text{C}$, and an exo-effect at $900\text{ }^{\circ}\text{C}$, and xonotlite by the appearance of endoeffects at $800 \dots 880\text{ }^{\circ}\text{C}$.

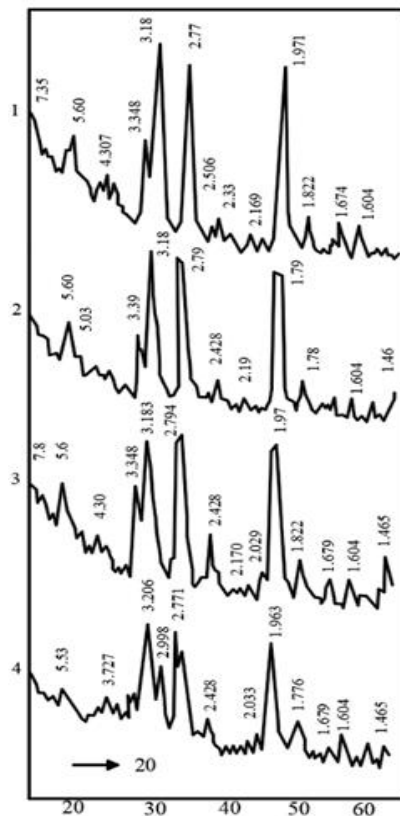
During hydration of glassy CS in the presence of Na_2CO_3 , regardless of the hardening conditions, in accordance with Figure 4a, the composition of the neoplasms is represented by CSH(I), gyrolite, pectolite and $\text{NaCa}(\text{CO}_3)_2 \cdot 2\text{H}_2\text{O}$ (d/n = 4.92; 3.16; 2.88; 2.65; 2.57; 2.5; 2.02; 1.89; 1.82 \AA).

The DTA curve in accordance with Figure 4b shows weak endothermic effects at 740 , 820 , and $960\text{ }^{\circ}\text{C}$, corresponding to the dehydration of CaCO_3 .

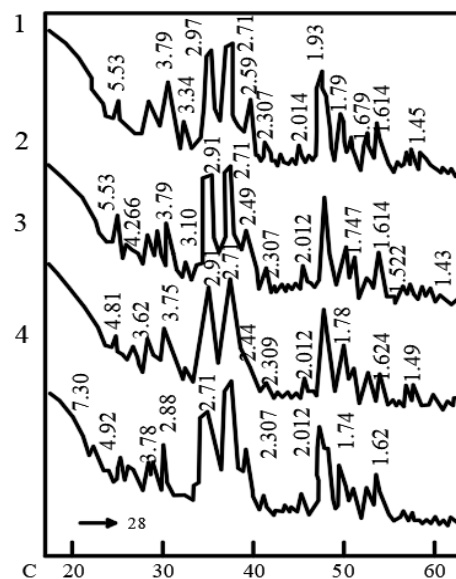
During the hydration of glass-like CS in the presence of Na_2SiO_3 , the composition of the hardening products is represented by compounds of cryptocrystalline structure: CSH(I), gyrolite, pectolite, and tobermorite. On the IR spectrogram, the presence of low-o basic calcium hydrosilicate is confirmed by the presence of absorption bands at 3365 , 1635 , 1173 , 1075 , 997 , 897 , and 524 cm^{-1} (Figure 4).

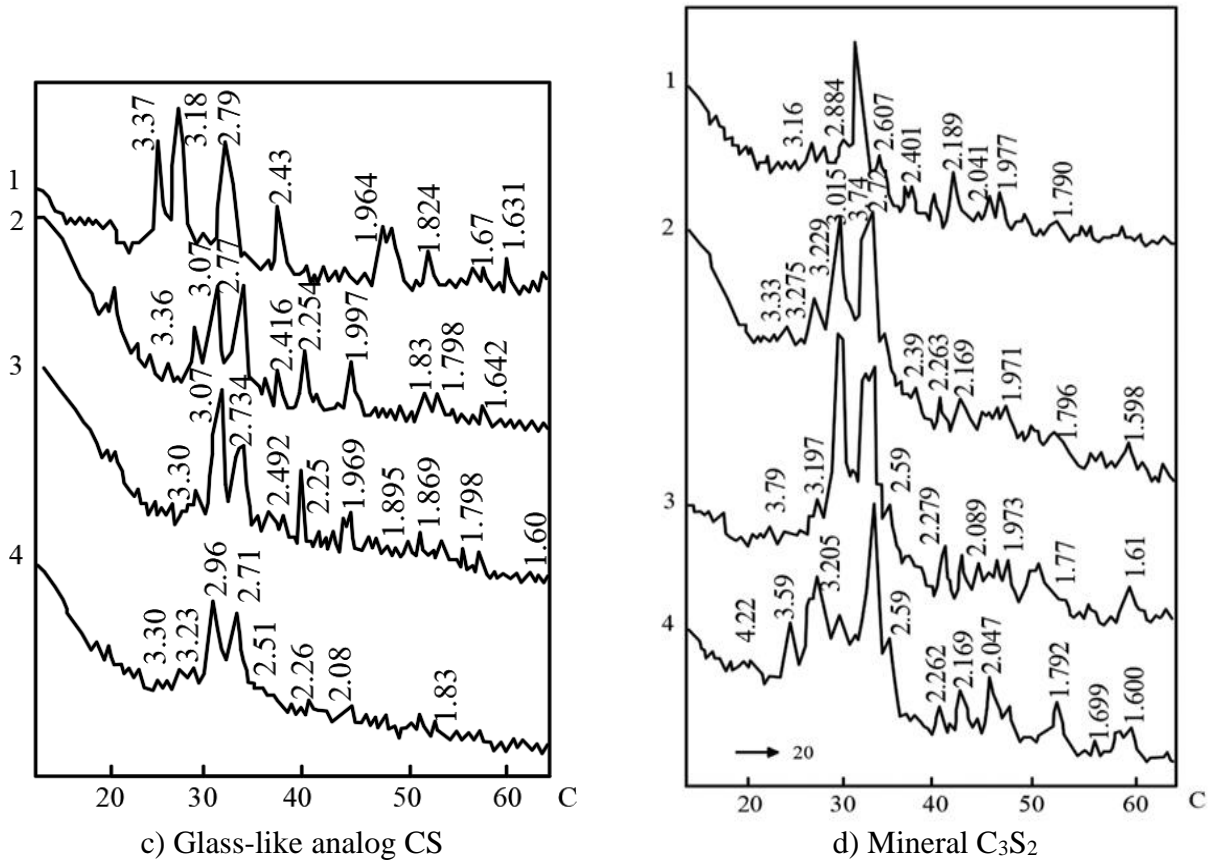
On the DTA curve, in accordance with Figure 4b, the main endothermic effect of tobermorite dehydration at $128\text{ }^{\circ}\text{C}$ is shifted toward low temperatures due to the introduction of Na^+ ions into its composition.

The thermogravimetric curve has no sharp fractures, and mass loss is observed in the temperature range of $20 \dots 800\text{ }^{\circ}\text{C}$. In the composition of the dehydration products at a temperature of $1000\text{ }^{\circ}\text{C}$, the predominance of $\beta\text{-CS}$ was noted and with an insignificant content in accordance with Figure 4b. During the heat and moisture treatment of CS, closed with a solution of Na_2SiO_3 , a clearer crystallization of low-base hydrosilicate phases is observed.

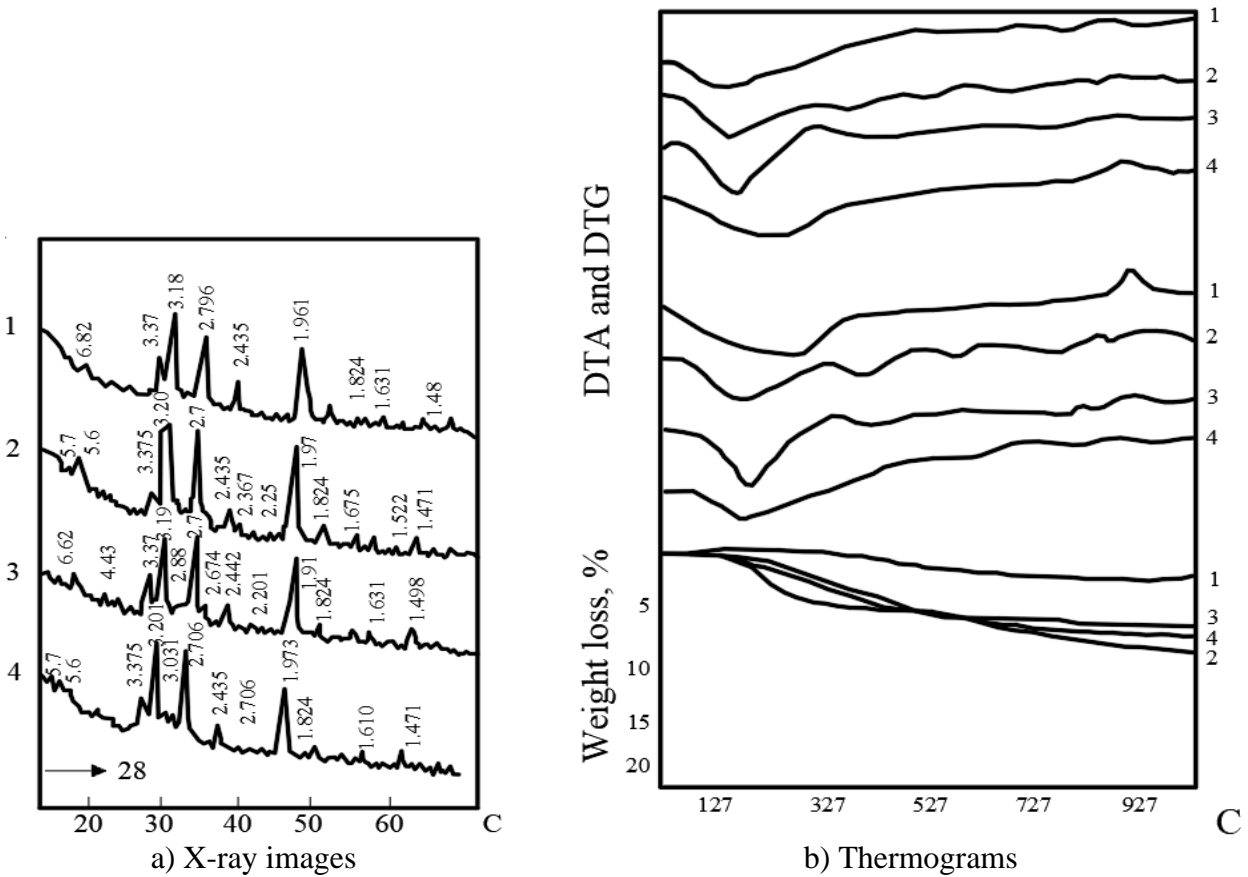


a) Mineral CS

b) Mineral C_3S_2

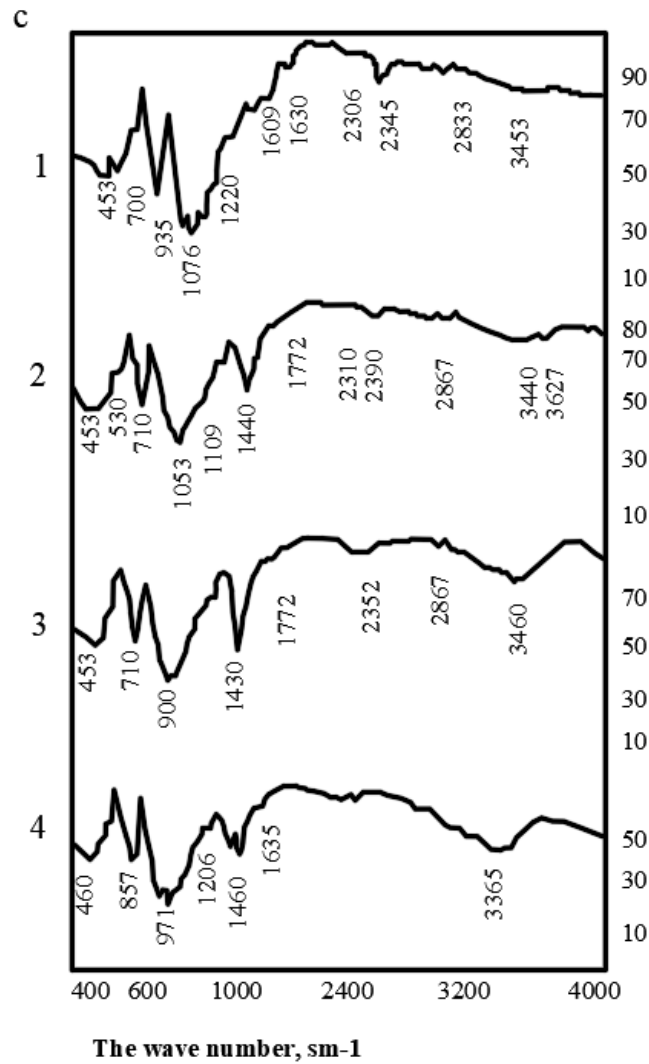


c) Glass-like analog CS
 d) Mineral C_3S_2
 Figure 3 – Radiographs of a stone: 1-with water; solutions: 2 - NaOH; 3 - Na_2CO_3 ; 4 - Na_2SiO_3 (heat and moisture treatment at $N = 95 \pm 5$ °C according to the regime 3+6+3+2)



a) X-ray images

b) Thermograms



c) IR spectrograms

Figure 4 – Results of the analysis of a stone based on a glass-like analog of CS closed with 1 – water; 2 – solution NaOH; 3 – solution Na_2CO_3 ; 4 – solution Na_2SiO_3 (28 days of storage in water)

Thus, the reduced strength and water resistance of an artificial stone based on glass-like CS, compared with the strength of a stone based on glass-like C_3S_2 , are due to the phase composition of hydration products represented by girolite, CSH(I) and pectolite, which do not possess crystallochemical affinity and belong to various categories of compounds.

According to the data of physico-mechanical tests given in Table 1, binders based on glass-like C_3S_2 hydrated with Na_2SiO_3 solution are characterized by the greatest hydraulic activity. The high strength (55...113 MPa) and its constant growth over time are due to the formation of epitaxially fused compounds in the hydration products: afvillite (monoclinic) and tobermorite-like hydrosilicates (orthorhombic) syngony.

Consequently, the most optimal conditions for the synthesis of strength artificial stone in the $\text{Na}_2\text{O}-\text{CaO}-\text{SiO}_2-\text{H}_2\text{O}$ system are created by hydration of binders of the glass-like analogue C_3S_2 with the formation of artificial stone, characterized by high rates of strength gain in the early stages of hardening and strength up to 125 MPa during long-term storage. This is due to the peculiarities of the structure of glassy calcium silicate, as well as the phase composition of hydration products: the ratio of gel-like and crystalline phases and the ability of hydrate compounds to form strong epitaxial accretions.

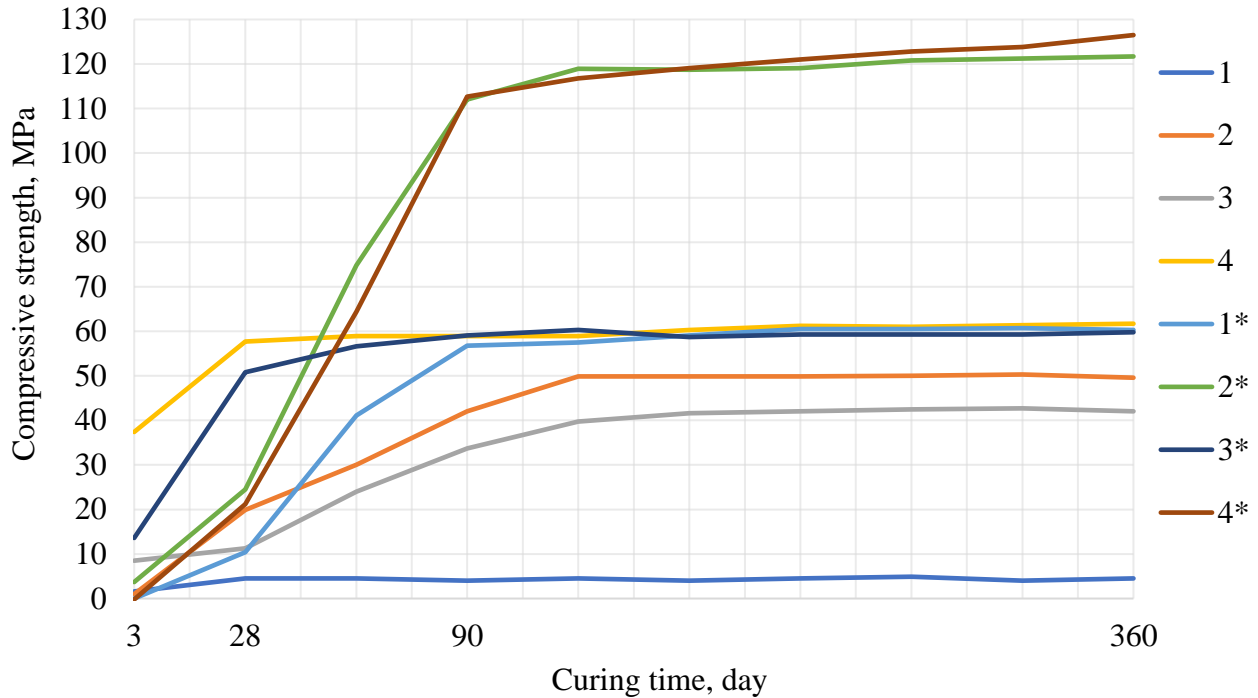


Figure 5 – Dependence of the strength of the binder based on C_3S_2 on the curing time with alkaline component: 1 – NaOH; 2 – Na_2CO_3 ; 3 – Na_2SiO_3 ; 4 – H_2O (*after aqueous storage)

Table 1 – Results of physical and mechanical tests of artificial stone based on hydrated glasses

Glass composition	Hardener	Compressive strength, MPa									
		After natural storage for a day				After water storage for a day				After heat and humidity treatment at a temperature of, °C	
		3	28	90	360	3	28	90	360	95	175
CS	H_2O	7.4	13.2	31.5	34.0	P	P	P	P	5.8	22.0
	NaOH	10.7	13.5	32.3	37.0	15.0	16.6	16.0	28.0	15.0	36.5
	Na_2CO_3	2.5	5.8	34.9	36.0	2.5	19.9	30.0	33.7	26.5	34.9
	Na_2SiO_3	23.2	34.8	69.7	72.0	33.0	35.7	45.0	69.0	50.0	66.0
C_3S_2	H_2O	1.0	1.5	3.3	5.8	2.5	15.0	59.4	63.0	1.5	30.0
	NaOH	5.0	20.0	43.0	48.0	12.5	49.5	57.0	62.0	20.0	35.0
	Na_2CO_3	8.0	12.5	35.0	42.0	5.0	21.5	113.2	121.0	35.0	55.0
	$Na_2O \cdot SiO_3$	37.5	57.5	59.4	63.0	33.0	55.0	113.5	125.0	62.5	71.0

Note: P is the soaking of the samples

4. Conclusions

1. The phase composition of hydration products plays a leading role in the formation of the structure of artificial stone of alkaline-alkaline-earth composition and determines its physical and mechanical properties. The analysis of the hydrate formation of the studied binder in the CS system shows that the most optimal conditions for the synthesis of stone strength with stable physical and mechanical properties are created when the hydration products contain a gel-like phase reinforced with hydrosilicates and hydroaluminosilicates of alkaline and alkaline-alkaline earth composition, characterized by a fibrous structure and having the ability to epitaxial fusion with each other, as well as the gel-like phase that they reinforce.

2. In the "calcium oxide – silicon oxide – alkaline component" system, high-strength stone (28 days – 53-58 MPa, 1 year – 125 MPa) is synthesized based on calcium silicates $1.5 \leq C/S \leq 2$

and the phase composition of hydration products is represented by low-basic hydrosilicates of the amitobermorite group, afvillite and alkaline-alkaline-earth hydrosilicates various degrees of crystallization ($\text{NaCO}_2 \text{SiO}_3\text{O}_8\text{OH}$; $\text{Na}_2\text{Ca}_8\text{Si}_5\text{O}_{26}\text{H}_{14}$).

Acknowledgment

This research was funded by the Science Committee of the Ministry of Science and Higher Education of the Republic of Kazakhstan (Grant No. BR21882292).

References

- [1] P. P. Budnikov and V. L. Pankratov, "Hydraulic activity of monocalcium silicate and helenite," in *Chemistry and technology of silicates*, Kiev: Naukova dumka, 1964, pp. 375–382.
- [2] P. P. Budnikov, B. C. Gorshkov, and T. A. Khmelevskaya, "Assessment of the astringent properties of slags according to their chemical and mineralogical composition," in *Chemistry and technology of silicates*, Kiev: Naukova dumka, 1964, pp. 446–457.
- [3] P. P. Budnikov and B. C. Gorshkov, "Investigation of hydrated synthetic minerals of alumina slags," in *Chemistry and technology of silicates*, Kiev: Naukova dumka, 1964, pp. 437–445.
- [4] S. Kucharczyk *et al.*, "Structure and reactivity of synthetic CaO–Al₂O₃–SiO₂ glasses," *Cem Concr Res*, vol. 120, pp. 77–91, Jun. 2019, doi: 10.1016/j.cemconres.2019.03.004.
- [5] S. Machida, K. Katsumata, K. Maeda, and A. Yasumori, "Effect of Vanadium Oxide on the Crystallization of CaO–Al₂O₃–SiO₂ Glass," *ACS Omega*, vol. 8, no. 9, pp. 8766–8772, Mar. 2023, doi: 10.1021/acsomega.2c08246.
- [6] S. Machida, K. Maeda, K. Katsumata, and A. Yasumori, "Microstructural Control of CaO–Al₂O₃–SiO₂ Glass Ceramics by Oxidation and Mixing with Nucleation Agents," *ACS Omega*, vol. 7, no. 37, pp. 33266–33272, Sep. 2022, doi: 10.1021/acsomega.2c03799.
- [7] M. M. Sychev, *Hardening of binders*. L: Stroyizdat, 1974.
- [8] B. K. Sarsenbayev, Z. A. Estemesov, J. T. Aimenov, N. B. Sarsenbayev, and A. J. Aimenov, *Slag-alkali binding concretes*. Shymkent, 2016.

Information about authors:

Bakhytzhhan Sarsenbayev – M. Auezov South Kazakhstan University, Shymkent, Kazakhstan, stroitelstvo_uku@mail.ru

Sultan Auyesbek – M. Auezov South Kazakhstan University, Shymkent, Kazakhstan, sultan_067@mail.ru

Meiram Begentayev – Kazakh National Research Technical University named after K. Satpayev, Almaty, Kazakhstan, m.begentayev@satbayev.university

Nuraly Sarsenbayev – M. Auezov, South Kazakhstan University, Shymkent, Kazakhstan, nurali777@mail.ru

Erkin Khaltursunov – Turin Polytechnic University in Tashkent, Tashkent, Uzbekistan, e.khaltursunov@polito.uz

Gaukhar Sauganova – M. Auezov, South Kazakhstan University, Shymkent, Kazakhstan, stroitelstvo_uku@mail.ru

Author Contributions:

Bakhytzhhan Sarsenbayev – concept, editing, drafting.

Sultan Auyesbek – data collection, testing, modeling.

Meiram Begentayev – editing the article and raising funds.

Nuraly Sarsenbayev – methodology, resources, analysis.

Erkin Khaltursunov – analysis, interpretation, modeling.

Gaukhar Sauganova – visualization, interpretation, methodology.

Conflict of Interest: The authors declare no conflict of interest.

Use of Artificial Intelligence (AI): The authors declare that AI was not used.

Received: 12.08.2024

Revised: 28.09.2024

Accepted: 29.09.2024







Published: 30.09.2024



Copyright: © 2024 by the authors. Licensee Technobius, LLP, Astana, Republic of Kazakhstan. This article is an open access article distributed under the terms and conditions of the Creative Commons Attribution (CC BY-NC 4.0) license (<https://creativecommons.org/licenses/by-nc/4.0/>).



Research of technological parameters for producing thermal insulating arbolite based on developed slag alkali binders

 Kuanysh Imanaliyev¹,  Baurzhan Amiraliyev^{1,*},  Kenzhebek Akmalaiuly²,
 Erzhan Kuldeyev²,  Elmurad Yunusaliyev³,  Zhambul Aymenov¹

¹M. Auezov South Kazakhstan University, Shymkent, Kazakhstan

²Kazakh National Research Technical University named after K.I. Satpayev, Almaty, Kazakhstan

³Ferghana Polytechnic Institute, Fergana, Uzbekistan

*Correspondence: badam777@imnbox.ru

Abstract. The paper presents the results of studies of an arbolite block made from rice husks. Granulated blast furnace slag of «Qarmet» OJSC and Dzhabul phosphorus slag were used as slag-alkali binders. The resulting material was examined for basic thermal and mechanical characteristics. As a result, it was found that the adhesion strength of the developed slag-alkali binders with rice husks exceeds the adhesion strength of Portland cement with the latter by 1.40 - 4.08 times, where slag-alkaline arbolite was obtained based on rice husks with an average density of 450-800 kg/m³ and a strength of 0.6 – 3.41 MPa. The frost resistance of the developed wood concrete compositions ranges from 15 to 30 cycles of alternating freezing and thawing. The results of this study can be used in the future when designing energy-efficient buildings.

Keywords: arbolite, rice husks, strength, slag, binders, slag-alkaline arbolite.

1. Introduction

Recently, cheaper construction methods have begun to be introduced in the construction industry, characterized not only by low cost, but also by relatively quick installation, minimal use of lifting equipment, a minimum range of materials used, and most importantly, low heat loss through the building envelope [1], [2], [3]. Such materials also include arbolite i.e., wood concrete [4], [5], [6].

A great contribution to the study and improvement of wood concrete production was made by domestic and foreign scientists, who, based on their research, emphasized the positive qualities of this material. The author Matyeva A.K. in her work [7] considers the technology of obtaining weather-resistant arbolite from chopped straw, where as a result arbolite was obtained with thermal conductivity qualities of the thermal interface thermal conductivity index equal to 0.07–0.09 W/(M K)*, which is 5 times better compared to burnt brick and strength from 1.8 to 4.0 MPa. In work [8], the authors carried out a simulation using the ANSYS software package of the effect on the thermal conductivity value of the pore content in arbolite blocks, where pores with content from 1.5% to 20% and the structure of the fibers in various directions were considered. However, the fiber structure also showed a significant difference from 8.16% to 15.33% depending on the direction of the fibers. In [9], the authors studied the effect of humidity on the strength characteristics of wood concrete, where they showed that wood concrete shows the greatest strength in its natural state. Thus, the previously conducted studies highlight the relevance of the direction, as well as the need to continue research in this direction.

The purpose of the work is to develop a technology for obtaining arbolite and its efficient production based on the optimization of the composition of slag-catching binders by processing granulated phosphorus and blast furnace slags with various technogenic modifiers.

2. Methods

The following were used as the main raw materials of slag-alkaline binders.

2.1 Aluminosilicate component of the slag-alkaline binder

The granulated blast furnace slag of JSC “Qarmet” (GBFS) was used (Table 1) [10].

The granulated blast furnace slag (GBFS) used in the research had the following chemical composition, with mass proportions of, %: CaO – 40.46; Al₂O₃ – 14.12; MgO – 7.97; SiO₂ – 36.08; TiO₂ – 0.99; BaO – 0.32; MnO – 0.33.

The Dzhambul phosphorus slag (PGS) was used (Table 1) [10]. Phosphorus slag had the following chemical composition, with mass proportions of, %: SiO₂ – 42.71; Al₂O₃ – 2.54; Fe₂O₃ – 0.25; CaO – 45.92; MgO – 3.24; P₂O₅ = 2.25; SO₃ – 0.5; puncture loss – 0.07.

Table 1 – Main physical characteristics of starting materials

Physical characteristics	Unit of measurement	PGS	GBFS
Bulk Density	kg/m ³	1210	1190
Density	g/cm ³	2.8	2.92
Basicity module	M _b	1.09	0.96
Activity module	M _a	0.06	0.39
Quality coefficient	C _q	1.2	1.68

2.2 Alkaline component of slag-alkaline binder

The following were used as an alkaline component:

- an aqueous solution of sodium silicate (liquid glass) with a silicate module M_s = 3, with a density of 1.1 ÷ 1.3 g/cm³;
- sodosulfate mixture, a waste from the production of caprolactam, the chemical composition of which is given in Table 2;
- sodium sulfide sludge, a waste product from the production of metallurgical chromium oxide (chrompic), the chemical composition of which is given in Table 3;
- caustic soda (NaOH).

Alkaline components were used in the form of an aqueous solution. The density of the alkaline component was changed by adding water, and the silicate module of sodium silicate was changed by adding an aqueous solution of sodium hydroxide.

Table 2 – Chemical composition of alkaline components

Name	Content of oxides and salts, mass%							
	SiO ₂	Na ₂ O	Al ₂ O ₃	Fe ₂ O ₃	Na ₂ CO ₃	Na ₂ SO ₄	NaCl	Impurities
Sodium silicate	73.2	24.4	1.5	0.07	-	-	-	0.82
Sodosulfate mixture	-	1-3	-	-	40-46	25-40	5-14	0.5-1

Table 3 – Chemical composition of chrompic

Na ₂ S ₂ O ₃	Na ₂ SO ₃	Na ₂ CO ₃	Na ₂ S	Cr ₂ O ₃
82.5-85.4	6.8-8.1	6.0-7.2	1.0	1.0

2.3 Organic filler

Rice husk was used as an organic filler, which is a waste of Akmarzhan JSC in Kyzylorda, formed during the technological processing of raw rice and meeting the requirements of [11] (Figure 1). The physical properties of rice husk are given in Table 4, and the fractional composition in Table 5.



Figure 1 – Rice husk

Table 4 – Physical properties of rice husk

Properties	Unit of measurement	Indicators
Bulk Density	kg/m ³	120
Natural humidity	%	9
Water absorption by mass	%	up to 160
Compaction coefficient		up to 2.5

Compared to wood, rice husks contain higher levels of inorganic substances and protein compounds, while at the same time, only pentosans are present among hemicelluloses. In addition, the equilibrium humidity values are low, but the smoldering and combustion temperatures are elevated (800-1000 °C). Strength characteristics are presented in Table 6.

Table 5 – Fractional composition of rice husks

Name of organic filler	Residue type	Residues on a sieve with a hole, mm%				Bottom
		20	10	5	2.5	
Rice husk	partial	0	10	9	69	22
	full	0	10	19	88	

The water absorption value of rice husk as a function of time is shown in Figure 2.

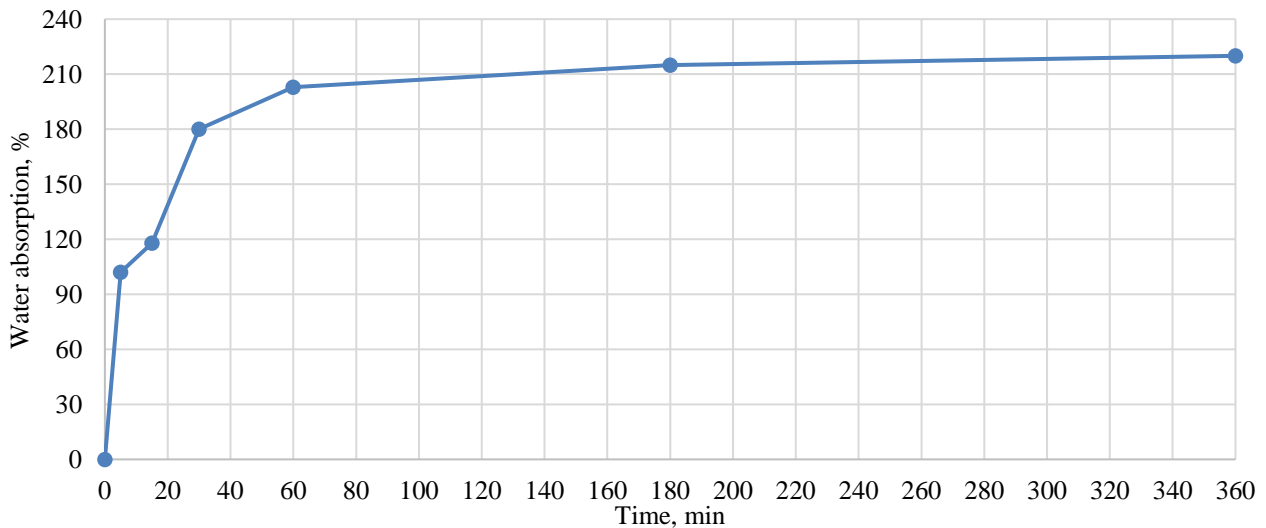


Figure 2 – Water absorption of rice husk as a function of time

Table 6 – Compositions and strength of the studied slag-alkaline binders

No.	Aluminosilicate component		Aqueous solution of alkaline component, %			ρ , g/cm ³	R _{compr.} , MPa
	Type of slag	Portland cement, %	Liquid glass	Chrompik	Sodosulfate mixture		
1	GBFS	-	8.8	1.95	-	1.28	90.9
2		-	5.9	3.9	-	1.25	66.0
3		-	5.9	-	3.33		84.4
4		-	-	7.8	-	1.2	20.0
5		5	-	4	-	1.1	15
6		5	-	-	3.5	1.25	26.5
7	PGS	-	5.9	-	3.33		87.2
8	slag	-	-	7.8	-	1.2	30
9		5	-	4	-	1.1	65
10		10	-	4	-	1.1	67
11*		6	-	-	8	1.0	36.9

Determination of technological parameters for their production and study of properties, where the main characteristics of the slag-alkali binder were determined in accordance with [12], [13], [14], [15], [16].

3. Result and Discussion

3.1 Study of the influence of technological parameters on producing arbolite

Existing technological lines for the production of arbolite structures are mainly based on standard equipment for the production of concrete using lightweight porous aggregates. However, organic filler of plant origin, due to its specific features, requires the introduction of adjustments to the technological stages of production. Rice husk, like other organic fillers, also has specific features, such as a loose and fragile structure, heterogeneity in the structure of the spatial frame, and high water absorption. It is also distinguished by its still low bulk density, significant anisotropic properties, high elastic-plastic, and many other characteristics. These listed properties must be taken into account when designing the composition and production technology of wood concrete, since the macro- and microstructure of the resulting material, which determine the strength indicators, depends on them.

In addition to the factors listed above, the strength of the wood-concrete largely depends on the properties and quantity of the starting materials for the preparation of the wood concrete mixture, on the methods of its preparation and installation, as well as on the hardening conditions and the environment in which the wood concrete will work.

Based on the above, our further research was aimed at studying the technological factors influencing the production of wood concrete with the proper quality in terms of strength, such as consumption of the alkaline component specific pressing pressure, and hardening conditions.

3.2 Effect of compaction coefficient on strength

When forming the structure of wood concrete, the compaction process plays an important role, since the strength and average density of the resulting material depends on the degree of compaction.

Due to the anisotropy of the properties and the low average bulk density of the organic filler, compaction of the wood-concrete mixture cannot be carried out by conventional vibration. In the practice of producing arbolite products, to compact the arbolite mixture, methods of power vibration rolling, roller vibrating rolling, pressing, and vibrating under load are used. Manual tamping is also used, but the latter is very labor-intensive. Of the listed methods, vibration with a weight has found wide application. This method allows, due to vibration, to reduce the specific

pressing pressure, and on the other hand, the use of molds with locking lids, since after removing the load, the compacted arbolite mixture is deformed back, which leads to disruption of the structure of the material.

Also, the progressive technology for manufacturing arbolite products includes the press method of molding an arbolite mixture with subsequent batch formation on a vertical conveyor of a molding station.

One of the important technological factors that determine the properties of a material is the coefficient (degree) of compaction, i.e., the ratio of the volume of the mixture in the loosely poured state to the volume of the molded material.

When studying the effect of the compaction coefficient of the wood-concrete mixture on strength, we used the composition of the wood concrete mixture in the ratio of components, mass, part: aluminosilicate component: rice husk: alkaline component = 1: 0.69: 0.71. In order to prevent reverse deformation of the samples, we used forms that allowed us to fix the volume of the sample. Fixation in a stationary state improves the contact interaction of the filler components with the binder, thereby developing the effect of contact hardening of the wood-concrete mixture.

The results obtained (Fig. 3) show that the strength of arbolite samples depends on the compaction coefficient of the mixture. Accordingly, with an increase in the compaction coefficient, the strength of the samples increases. Whereas, the samples molded without load had a strength of only 0.047 MPa (at $C_{\text{compaction}} = 1$), increasing $C_{\text{compaction}}$ to 1.5 made it possible to obtain wood concrete with a strength of 0.55 MPa, while the specific pressing load was equal to 0.012 MPa. A further increase in the specific pressing pressure by 0.076 MPa (at $C_{\text{compaction}} = 2$) led to an increase in the strength of the wood-concrete by 0.95 MPa. In this case, a dense packing of the constituent components of the arbolite mixture occurs, since the filler particles, being suspended in the arbolite mixture, during compaction tend to occupy a position in which the direction of the large size of each particle becomes parallel to the layers of the mixture.

From the results obtained it follows that an increase in the specific pressing pressure from 0.088 to 0.29 MPa led to an increase in the strength of arbolite samples by only 0.64 MPa.

When conducting research, it was revealed that with an increase in the liquid added to the mixture, it is also possible to reduce the specific pressing pressure, but at the same time, excess liquid flows out of the mold and, due to this, the homogeneity of the material is disrupted.

Based on the results obtained, we can make a preliminary conclusion that with increasing $C_{\text{compaction}}$, the strength of the arbolite samples increases, as a result of which the density also increases, since although the ratio of the components of the wood-concrete mixture was constant, the actual consumption of materials per 1m^3 of products also increases.

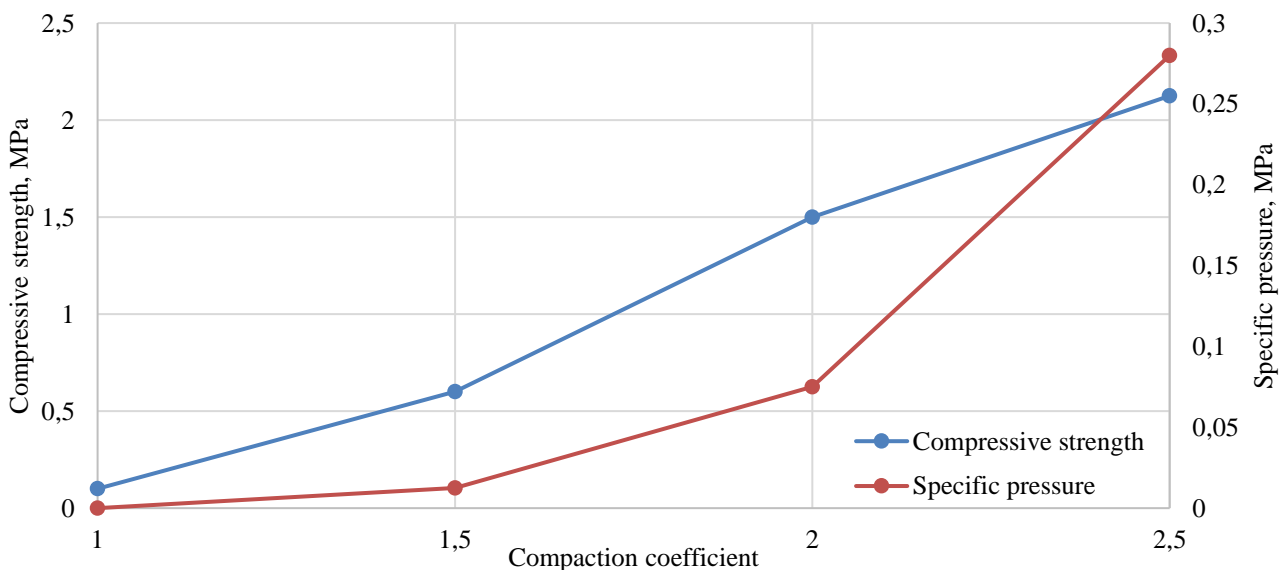


Figure 3 – The influence of the compaction coefficient on the strength of arbolite and on the specific compaction pressure of the mixture

3.3 Influence of hardening conditions on strength

Wood concrete consists mainly of two materials that are opposite in nature, the first is an organic aggregate that requires dry conditions and the second is a mineral binder that requires moisture and a certain temperature for the hydration reaction to occur. Therefore, the hardening of wood concrete products is an important technological operation in its production. Finding the optimal heat treatment regime for products will largely determine the strength and other indicators of products. Therefore, studying hardening processes and choosing optimal ways to accelerate them is a necessary task.

In the traditional technology for the production of wood concrete based on Portland cement, to accelerate its hardening, it is recommended to carry out heat treatment at a temperature of 40°C and a relative humidity of 50-60%. To accelerate the hardening of arbolite samples and determine the optimal heat treatment modes, staged experiments were carried out. The results obtained were analyzed and the following were established:

- that for the developed compositions, slag-alkali wood concrete on rice husks, the optimal heat treatment temperature is 70°C with isothermal exposure according to the 3+3+8+3 scheme. In further studies, to accelerate the hardening of arbolite samples, we used this heat treatment mode.

3.4 Study of the construction and technical properties of slag-alkali wood concrete on rice husks

The basic properties of slag-alkali wood concrete on rice husks, including strength, water absorption and swelling, and frost resistance, have been studied.

3.4.1 Change in strength over time

Studies of these properties were carried out on the developed compositions of slag-alkaline wood concrete on rice husks (Table 7).

Table 7 – Compositions and properties of slag-alkali wood concrete on rice husks

Slag-alkali binder's composition No.	Material consumption per 1 m ³ of wood concrete						Compressive strength, 28 days, MPa	Average density of wood concrete, kg/m ³
	Binder components					Rice husk, kg		
	Aluminosilicate		Alkaline component					
Type of slag	Quantity, kg	Type	Density, g/cm ³	Quantity, l				
1		250			200	150	0.5	465
2		350			225	150	1.6	572
3	Karaganda granulated blast furnace slag	350	Liquid glass + chrompic	1,28	270	240	2.8	678
4		500			315	240	3.6	825
5		350			225	150	1.4	552
6		500			315	240	3.4	805
7		250	Liquid glass + Sodosulfate	1,25	200	150	1.1	459
8	Electrothermal-phosphorus slag	500	mixture		315	240	1	800
9		350	Chrompic	1,1	225	150	1	442
10		500	Sodosulfate	1	315	240	2	785
11		350	mixture		315	240	1.8	635

Note: In compositions 10-11, the aluminosilicate component contains 5% Portland cement. Composition 11 was mixed with water.

The tests were carried out on samples that had hardened under natural conditions after heat treatment at the age of 1; 28; 90; and 180 days. It should be noted that the heat treatment was carried out at high humidity of the environment, created due to the release from moisture filler at a temperature of 70 °C. To do this, the forms with the samples were tightly closed.

In this mode, a kind of “microclimate” is created inside the mold, which has a beneficial effect on the hardening processes of the binder, which, as is known, is hydraulic.

Tests have shown that with prolonged hardening, the strength of wood concrete increases, which indicates the continuation of hydration processes and an increase in the strength of the slag-alkaline binder stone.

The research results showed that the most intensive increase in the strength of wood concrete based on slag-alkaline binder is observed up to 28 days of age (Figure 4). At the same time, the increase in strength ranges from 12 to 25%. This increase can be explained by the fact that during this period the wood concrete is still in a wet state. The existing alkali in the alkaline component, extinguished by the organic filler, along with evaporating water, gradually migrates from the filler, as a result of which the hydration processes of the slag-alkaline binder deepen during subsequent hardening. At the same time, the density of the binding frame of the slag-alkali wood concrete increases, moisture losses decrease, and an increase in strength is observed over time. During the hardening period from 28 to 180 days, the moisture content of the wood-concrete is stabilized and its strength is also stabilized for almost all compositions, with the increase in strength ranging from 2 to 13%.

3.4.2. Water absorption and swelling

The water absorption test of arbolite samples was carried out on samples with rib dimensions of 10x10x10 cm, at normal atmospheric pressure.

The results obtained show (Figure 5) that the water absorption rate strongly depends on the density of wood concrete, which is associated with the content of binder and rice husk. Moreover, the lower the average density of wood concrete, the greater its water absorption rate. An increase in average density leads to a decrease in water absorption. Thus, arbolite samples with an average density of 500 kg/m^3 have this indicator equal to 89% by weight. This is explained by the fact that the organic filler - rice husk - has high water absorption. An increase in the density of wood concrete by 350 kg/m^3 led to a decrease in water absorption by 57% and amounted to 32%, respectively. It should be noted that the samples containing sand have the lowest water absorption.

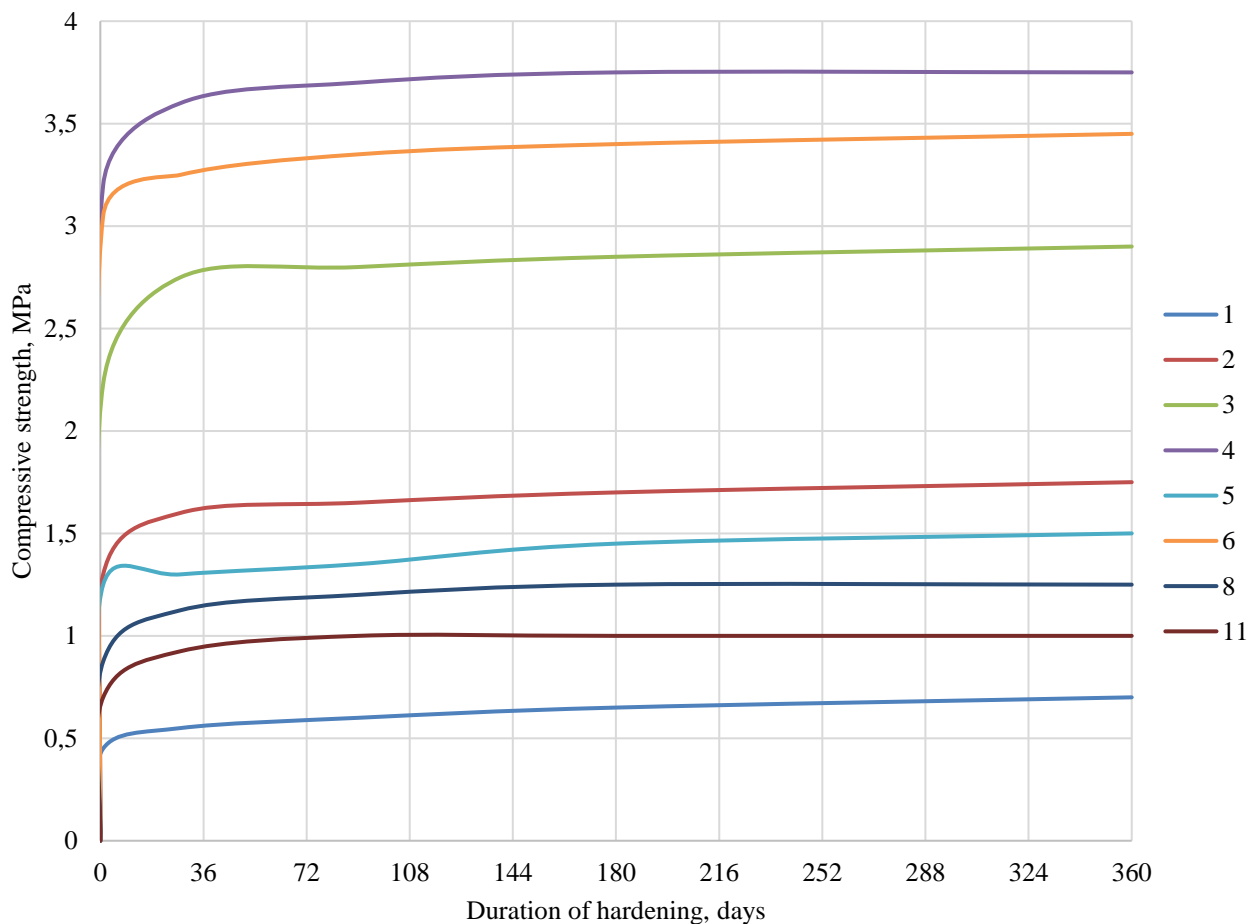


Figure 4 – Change in the strength of slag-alkali wood concrete on rice husks by time (the numbers of the compositions are according to the Table 7)

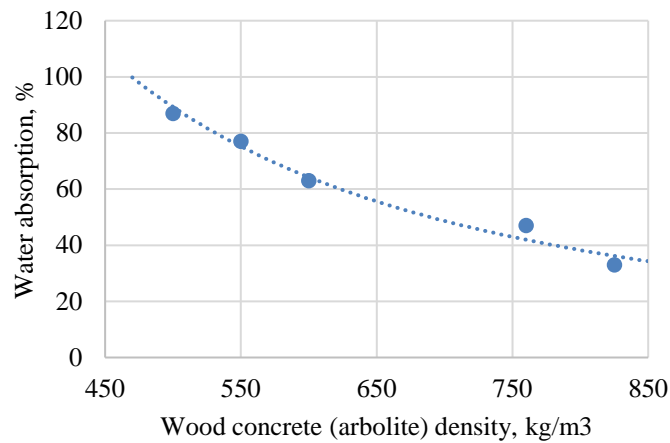


Figure 5 – Dependence of water absorption of slag-alkaline wood concrete on average density

The water absorption of wood concrete and structures can be reduced by protecting its open surfaces with various films and coatings. A protective layer of cement-sand mortar with a composition of 1:5 and a thickness of up to 10 mm reduces the water absorption of wood concrete by up to two times.

The results obtained from the study of linear swelling of samples made of slag-alkali wood concrete on rice husks in a water-saturated state show that they also depend on the density of wood concrete and range from 0.98 to 1.75%. It should be noted that the lowest swelling rate is characteristic of samples with the lowest content of organic filler.

3.4.3. Frost resistance

The frost resistance of slag-alkali arbolite on rice husks was determined on sample cubes with edge dimensions of 10x10x10 cm. The duration of freezing at a temperature of -20 °C was 4 hours. Thawing time at a temperature of 20 °C is 4 hours.

Tests of the frost resistance of slag-alkaline arbolite have shown (Table 8) that the frost resistance of the latter depends on its composition and ranges from 15 to 30 cycles of alternating freezing and thawing. The developed wood concrete meets the requirements in terms of frost resistance.

Table 8 – Frost resistance of slag-alkaline arbolite

Com position No. according to table. 7	Frost resistance coefficient through, cycles				Frost resistance, cycle
	15	25	30	40	
2	0.83	0.65	0.35		15
3	0.86	0.78	0.71		15
6	0.94	0.85	0.75		25
7	0.98	0.92	0.87	0.76	30
12	0.97	0.87	0.78	0.69	25

4. Conclusions

This paper presents technological solutions for obtaining slag-alkali arbolite on rice husks, allowing the use of industrial and agro-industrial waste, which lead to savings in expensive raw materials and the solution of economic and environmental issues.

The main results, practical recommendations obtained personally by the author, in the course of research work are as follows:

1. The possibility of obtaining slag-alkali arbolite on rice husks, with an average density of 450-800 kg/m³ and a strength of 0.6-3.41 MPa, is theoretically substantiated and experimentally

proven due to the implementation of the properties of highly reactive slag-alkali binder and optimization of the technology for its production, ensuring high technology and construction and technical properties.

2. It was established that the adhesion strength of the developed slag-alkali binders with rice husks exceeds the adhesion strength of Portland cement with rice husks by 1.40 - 4.08 times. The highest adhesion strength values are demonstrated by binders sealed with a sulfate-containing alkaline component in combination with liquid glass, which are 0.18-0.21 MPa.

3. It has been established that the amount of the alkaline component introduced during the preparation of the arbolite mixture depends on the ratio of rice husk and aluminosilicate component. A graphical dependence of the effect of the alkaline component consumption on the ratio of rice husk and aluminosilicate component has been experimentally determined and derived.

4. The developed arbolite compositions on a slag-alkaline binder increase their strength over time. A more intensive gain in strength is observed up to the age of 28 days. In this case, the strength increase is from 12 to 25%. The linear swelling of slag-alkaline arbolite on rice husk in a water-saturated state depends on the density of the arbolite and is from 0.98 to 1.75%. The lowest swelling value is characteristic of samples with the lowest content of organic filler. The frost resistance of the developed arbolite compositions is from 15 to 30 cycles of alternating freezing and thawing. They have high weather resistance.

5. A technology for the production of slag-alkaline arbolite on rice husks has been developed, which allows, due to the use of the developed slag-alkaline binder compositions, to save time and energy costs of production due to accelerated hardening of arbolite products. At the same time, the production cycle of products is reduced to 3 times, and energy costs to 1.3-1.4 times compared to the traditional technology of arbolite production on Portland cement binder. In addition, the production of slag-alkaline binders also allows saving energy and natural mineral raw materials.

Acknowledgments

This research was funded by the Science Committee of the Ministry of Science and Higher Education of the Republic of Kazakhstan (Grant No. BR21882292 – “Integrated development of sustainable construction industries: innovative technologies, optimization of production, effective use of resources and creation of technological park”).

References

- [1] T. Samoilova, M. Rakhimov, G. Rakhimova, and N. Zhangabay, “Effect of heat treatment of expanded polystyrene concrete on its compressive strength,” *Technobius*, vol. 4, no. 2, p. 0059, Jun. 2024, doi: 10.54355/tbus/4.2.2024.0059.
- [2] R. Lukpanov, D. Dyusseminov, A. Altynbekova, Z. Zhantlesova, and T. Seidmarova, “Research of foam concrete quality by two-stage foam injection method in comparison with classical foam concrete,” *Technobius*, vol. 4, no. 1, p. 0052, Mar. 2024, doi: 10.54355/tbus/4.1.2024.0052.
- [3] N. Zhangabay, S. Bugarova, I. Baidilla, and A. Tagybayev, “MODELING OF THERMAL RESISTANCE OF THE DEVELOPED EXTERNAL ENCLOSING STRUCTURES WITH AN AIR LAYER,” *Bulletin of Kazakh Leading Academy of Architecture and Construction*, vol. 88, no. 2, pp. 178–191, Jun. 2023, doi: 10.51488/1680-080X/2023.2-19.
- [4] B. Martínez, V. Mendizabal, M. B. Roncero, E. Bernat-Maso, and L. Gil, “Towards sustainable building solutions: Development of hemp shiv-based green insulation material,” *Constr Build Mater*, vol. 414, p. 134987, Feb. 2024, doi: 10.1016/j.conbuildmat.2024.134987.
- [5] M. Dlimi, R. Agounoun, I. Kadiri, R. Saadani, and M. Rahmoune, “Thermal performance assessment of double hollow brick walls filled with hemp concrete insulation material through computational fluid dynamics analysis and dynamic thermal simulations,” *e-Prime - Advances in Electrical Engineering, Electronics and Energy*, vol. 3, p. 100124, Mar. 2023, doi: 10.1016/j.prime.2023.100124.
- [6] H. G. Şahin, A. Mardani, S. Özen, and A. Emin, “Utilization of high-range water reducing admixture having air-entraining agents in cementitious systems,” *Journal of Building Engineering*, vol. 64, p. 105565, Apr. 2023, doi: 10.1016/j.jobee.2022.105565.
- [7] A. K. Matyeva, “MANUFACTURE OF MODIFIED ARBOLIT FROM LOCAL RAW MATERIALS: OPTIMIZATION OF COMPOSITION AND PROPERTIES OF RAW MATERIAL COMPONENTS,” *The*

Russian Automobile and Highway Industry Journal, vol. 16, no. 3, pp. 352–365, Jul. 2019, doi: 10.26518/2071-7296-2019-3-352-365.

- [8] N. Zhangabay, D. Chepela, T. Tursunkululy, A. Zhangabay, and A. Kolesnikov, “Analysis of the effect of porosity on thermal conductivity with consideration of the internal structure of arbolite,” *Construction materials and products*, vol. 7, no. 3, pp. 4–4, May 2024, doi: 10.58224/2618-7183-2024-7-3-4.
- [9] A. N. Yagubkin, V. V. Bozylev, and D. S. Zelenkevich, “Vliyaniye vlazhnosti na vodostoykost’ i dolgovechnost’ arbolitovykh izdeliy,” *Bulletin of Polotsk State University*, vol. 16, pp. 60–63, 2012.
- [10] A. S. Kurtaev and Z. A. Estemesov, *Kompozitsionnyye materialy na osnove neorganicheskikh vyazhushchikh veshchestv*. Kiev: IMP, 1998.
- [11] *TU-822-11-78 Rice husk*. 1979, p. 7.
- [12] *GOST 310.1-76 Cements. Methods for determining grinding fineness*. 1976.
- [13] *GOST 310.2-76 Cements. Test methods*. 1976.
- [14] *GOST 310.3-76 Cements. Methods for determining normal density, setting time and uniformity of volume change*. 1976.
- [15] *GOST 310.4-76 Cements. Methods for determining bending and compressive strength*. 1976.
- [16] *GOST 25820-83 Concrete. Methods for determining water absorption*. 1983.

Information about authors:

Kuanysh Imanaliyev – M. Auezov South Kazakhstan University, Shymkent, Kazakhstan, kuanish.69@mail.ru

Baurzhan Amiraliyev – M. Auezov South Kazakhstan University, Shymkent, Kazakhstan, badam777@inbox.ru

Kenzhebek Akmalaiuly – Kazakh National Research Technical University named after K.I. Satpayev, Almaty, Kazakhstan, kakmalaev@mail.ru

Erzhan Kuldeyev – Kazakh National Research Technical University named after K.I. Satpayev, Almaty, Kazakhstan, e.kuldeyev@satbayev.university

Elmurad Yunusaliyev – Ferghana Polytechnic Institute, Fergana, Uzbekistan, e.yunusaliyev@ferpi.uz

Zhambul Aymenov – M. Auezov South Kazakhstan University, Shymkent, Kazakhstan, zhambul_ukgu@mail.ru

Author Contributions:

Kuanysh Imanaliyev – concept, resources, supervision, analysis.

Baurzhan Amiraliyev – data collection, testing, concept, methodology.

Kenzhebek Akmalaiuly – funding acquisition, drafting, editing.

Erzhan Kuldeyev – resources, drafting, editing.

Elmurad Yunusaliyev – analysis, visualization, data processing.

Zhambul Aymenov – methodology, drafting, interpretation.

Conflict of Interest: The authors declare no conflict of interest.

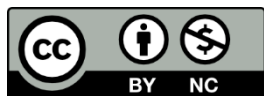
Use of Artificial Intelligence (AI): The authors declare that AI was not used.

Received: 20.08.2024

Revised: 28.09.2024

Accepted: 29.09.2024

Published: 30.09.2024



Copyright: © 2024 by the authors. Licensee Technobius, LLP, Astana, Republic of Kazakhstan. This article is an open access article distributed under the terms and conditions of the Creative Commons Attribution (CC BY-NC 4.0) license (<https://creativecommons.org/licenses/by-nc/4.0/>).